Robust Transmit Beamforming With Artificial Redundant Signals for Secure SWIPT System Under Non-Linear EH Model

Yang Lu, Ke Xiong, *Member, IEEE*, Pingyi Fan, *Senior Member, IEEE*, Zhangdui Zhong, *Senior Member, IEEE*, and Khaled Ben Letaief, *Fellow, IEEE*

***Abstract*— This paper investigates the secure transmit design for simultaneous wireless information and power transfer system under the non-linear energy harvesting (EH) model, where a transmitter sends confidential information and transfers energy to multiple information receivers (IRs) and EH receivers (ERs) with the existence of multiple eavesdroppers (Eves). To prevent confidential information leakage, multiple artificial redundant signals (MARSs) are embedded in the transmit signals. The goal is to minimize the total transmit power by jointly optimizing transmit beamforming vectors and the covariance matrixes of MARSs, such that the minimal information rate and EH requirements at IRs and ERs are guaranteed while making the received signal-to-Interference ratio at ERs and Eves lower than their information decoding thresholds. Both the non-robust and the robust designs are studied. For the non-robust design, the optimal solution is derived. For the robust design, an approximate optimal solution is obtained by using Gaussian randomization procedure. Simulation results show that compared with traditional non-MARS-aided beamforming design, our proposed design is superior in terms of the total required transmit power. It also shows that employing the non-linear EH model can avoid false output power at the ERs and/or save power at the transmitter.**

***Index Terms*— Secure transmission, SWIPT, non-linear energy harvesting model, artificial noise, artificial redundant signals.**

Manuscript received July 17, 2017; revised November 5, 2017; accepted December 20, 2017. Date of publication January 12, 2018; date of current version April 8, 2018. This work was supported in part by the Key Program of the National Natural Science Foundation of China (NSFC) under Grant U1334202, in part by the General Program of NSFC under Grant 61671051, in part by the Youth Fund Program of NSFC under Grant 61602034, in part by the Innovation Research Group Science Fund Project of NSFC under Grant 61621091, and in part by NFSC Outstanding Youth under Grant 61725101. The associate editor coordinating the review of this paper and approving it for publication was D. W. K. Ng. *(Corresponding author: Ke Xiong.)*

Y. Lu and K. Xiong are with the School of Computer and Information Technology, Beijing Jiaotong University, Beijing 100044, China, and also with the Beijing Key Laboratory of Traffic Data Analysis and Mining, Beijing Jiaotong University, Beijing 100044, China (e-mail: kxiong@bjtu.edu.cn.).

P. Fan is with the National Laboratory for Information Science and Technology, Tsinghua University, Beijing 100084, China, and also with the Department of Electronic Engineering, Tsinghua University, Beijing 100084, China.

Z. Zhong is with the State Key Laboratory of Rail Traffic Control and Safety, Beijing Jiaotong University, Beijing 100044, China, and also with the Beijing Engineering Research Center of High-Speed Railway Broadband Mobile Communications, Beijing Jiaotong University, Beijing 100044, China.

K. B. Letaief is with the School of Engineering, The Hong Kong University of Science and Technology, Hong Kong (e-mail: eekhaled@ece.ust.hk).

Color versions of one or more of the figures in this paper are available online at http://ieeexplore.ieee.org.

Digital Object Identifier 10.1109/TWC.2018.2790384

I. Introduction

A. Background

In THE last decade, simultaneous wireless information and power transfer (SWIPT), which combines the wireless electric power transfer (WPT) and wireless information transfer (WIT), has drawn increasing attention [1]–[3]. With SWIPT, the receiver is able to decode information or convert received radio frequency (RF) signals into direct current (DC) power according to its own need. Therefore, SWIPT is expected to prolong the operation time of devices in the low-power energy-constrained networks, e.g., wireless sensor networks (WSNs) and Internet of Things (IoTs) [4]–[6]. Different from traditional wireless communications, SWIPT integrates energy harvesting (EH) with communication devices, which enables wireless devices to scavenge energy from RF signals by their RF-EH circuits.

For the RF-EH circuit, one of its most important parameters is the RF-to-DC conversion efficiency factor, which is demonstrated by the ratio of the output DC power to the input RF power (i.e., the ratio of the harvested power to the received RF signal power). In most existing works, the *linear EH model* [7] was adopted, where RF-to-DC conversion efficiency was assumed to be independent of the input RF power level, which was described by a constant that takes the value in the interval $[0, 1]$. However, practical measurement results [8]–[14] indicated that non-linear elements, e.g., diode-connected transistors, in RF-EH circuits make the RF-to-DC conversion efficiency vary with the input RF power level, which shows *non-linear EH* behavior. To avoid the performance loss in practical systems, SWIPT systems should be designed based on the non-linear EH model rather than the linear one.

On the other hand, to improve the spectral and energy efficiency, SWIPT is often combined with multi-antenna techniques [7], [15], [16]. Multi-antenna SWIPT systems are able to provide different services to multiple receivers, including information decoding (ID) receivers (IRs) and EH receivers (ERs), over the same band frequency in one-time transmission. So far, a lot of issues have been addressed in multi-antenna SWIPT systems, where one of the most important issues is the secure information transmission problem [17], [18], because in future wireless systems, especially in customer IoT systems, more and more privacy

1536-1276 © 2018 IEEE. Personal use is permitted, but republication/redistribution requires IEEE permission.
See http://www.ieee.org/publications_standards/publications/rights/index.html for more information.

information will be delivered. That is, how to avoid the confidential information leakage to eavesdroppers (Eves) is of great significance. The secure transmission could be realized by secure beamforming design, where beam vectors are optimized to make the received SINR at each IR higher than a predefined threshold and at the same time make that at each ER and Eve lower than a secure threshold [19]. Latter, it was found that embedding the artificial noise (AN) in the transmit signals can further enhance the secrecy in multi-antenna SWIPT system [20], [21]. Since AN signals also carry energy, it may also be used as a energy provider to transfer energy to ERs in SWIPT systems.

Besides AN, recently, the conception of redundant signals was proposed in [22], where for each IR, one beamformer is devoted to information signal while several additional "shaping beamformers" are used for randomly generating *multiple artificial redundant signals (MARSs)*. Since MARSs make the beamforming design satisfy an arbitrary number of shaping constraints, in this paper, we try to embed MARSs into the secure SWIPT to enhance the system performance. Note that traditional AN-aided beamforming designs only involve one artificial redundant signal (ARS), see e.g., [19]–[21], so they only can be regarded as a special case of the MARS-aided beamforming design.

B. Related Work and Motivation

In this paper, to inherit the advantages of SWIPT, multi-antenna technologies and MARSs, we focus on MARS-aided beamforming designs for multi-antenna SWIPT systems under the non-linear EH model. Our goal is to minimize the total required power by jointly optimizing transmit beamforming vectors and the covariance matrixes of MARSs, while satisfying the information rate requirement of each IR and the EH requirement of each ER and avoiding the information being intercepted by ERs and Eves. In order to highlight the novelty of this paper, it is worthy to emphasize the following differences between our work and existing ones [23], [25]–[32].

Firstly, in existing works, only one IR was considered (see e.g., [23]) or only the transmitter was equipped with multiple antennas (see e.g., [25]–[27]). Comparatively, this paper involves multiple receivers (i.e., IRs, ERs and Eves), and multiple antennas are equipped on both the transmitter and some receivers. Although, some recent work began to consider secure multi-user SWIPT MIMO channel, only common information broadcasting scenario was studied, where the inter-user interference was not involved, see e.g., [28]. In this paper, different IRs require different information from the transmitter and thus, the inter-user interference is considered. Besides, both single-antenna and multi-antenna Eves are involved in our work. Therefore, our considered system is more general.

Secondly, in all existing works related to secure SWIPT systems, traditional linear EH model was adopted, which mismatches the practical system and may lead to false optimization results of system configuration. To avoid the performance loss, this paper considers the non-linear EH model obtained with real data measurement [8]. Therefore, the study in this paper is much closer to practical systems.

Thirdly, in all existing works mentioned above, only the AN-aided beamforming design, i.e., single ARS case, was investigated. In this paper, both the single ARS-aided and the MARS-aided beamforming designs are studied. Moreover, the effect of MARSs are also discussed.

Fourthly, in most existing works (see e.g., [29], [30]), their goal was to maximize the system secrecy capacity, while this paper investigates the power minimization system design in order to meet the green communication requirements for future 5G. Although some works also discussed the power-minimization secure SWIPT system design, they considered either MISO channel or secure rate constraints, rather than the hybrid MIMO and MISO channel with QoS, EH and secure constraints.

Besides, compared with some existing works, see e.g., [31], [32], where only the non-robust design was investigated under the perfect CSI assumption. This paper investigates both the non-robust and the robust designs for MARS-aided SWIPT systems.

C. Contributions

The contributions of this paper are summarized as follows.

- A general SWIPT system is investigated in this paper, where a multi-antenna transmitter intends to send confidential information to multiple single-antenna IRs while transferring wireless energy to a group of multi-antenna ERs. Multiple energy-bearing MARSs are embedded in the transmit signals to prevent the interception of Eves and ERs.
- To meet green communication requirements, the power minimization problem is investigated under both perfect and imperfect CSI assumptions. Due to incorporating the MARSs and the non-linear EH model, the considered problem is non-convex and cannot be solved directly. For the perfect CSI case, an equivalent problem is solved and the optimal solution is derived by using semidefinition relaxation (SDR), where the rank-one solution is proved to be guaranteed by using Karush-Kuhn-Tucker (KKT) conditions. For the imperfect CSI case, the worst-case robust problem is presented and solved by a proposed solving approach based on SDR and S-procedure, and an approximate optimal solution is obtained by using Gaussian randomization procedure. The main purpose is to find the efficient solving approaches and some hidden relations of the system performance with these constraints for the secure SWIPT systems with the non-linear EH model and MARSs. Moreover, the computational complexity of the proposed non-robust and robust design approaches are also discussed.
- The effect of MARSs is discussed, which indicates that by employing MARSs, the total transmit power can be reduced under the same conditions once the number of the transmit antennas is larger than that of the transmit signals. Particularly, when the optimization problem associated with the system design is "linearized", the number

of MARSs has no effect on the optimal value when it is larger than 1.[1]

- Numerical results of the MARS-aided and the non-MARS aided beamforming designs, the non-robust and the robust beamforming designs, and the non-linear and the linear EH models are respectively presented and compared. It shows that our simulation results and theoretical ones match well. Moreover, compared with traditional non-MARS aided beamforming design, our proposed design requires less transmit power to achieve the same system performance, especially when limited degree of freedom (DoF) is achieved at the transmitter. Compared with traditional linear EH model, employing the non-linear EH model can avoid false output power at ERs or save power consumption at the transmitter, as the real RF-EH circuits are working in the non-linear output field rather than the linear one.

Note that the non-linear EH circuits make the feasible set of the considered problem much different from that associated with the linear EH model. That is, there exists a saturation region of the non-linear EH circuits, which restricts the maximum output DC power. Therefore, the feasible set associated with the non-linear EH model does not extend with increment of the EH power requirement infinitely.

This paper is organized as follows. Section II gives the system model description. Section III formulates the problem, solves it under both the perfect CSI and imperfect CSI assumptions, and analyzes the computational complexity of the presented solving approaches. Section IV discusses the effect of the MARSs. Simulation results are illustrated in Section V. Section VI concludes the paper.

Notations: Boldface lowercase and uppercase letters denote vectors and matrices, respectively. The set of n-by-m complex matrixes and complex Hermitian matrices are denoted by $\mathbb{C}^{n\times m}$ and $\mathbb{H}^{n\times m}$, respectively. For a complex number a, $|a|$ denotes the modulus. For a vector $\mathbf{a}$, $\|\mathbf{w}_n\|_2$ denotes the Euclidean norm. The conjugate transpose, rank, trace and determinant of the matrix $\mathbf{A}$ are denoted as $\mathbf{A}^H$, Rank $(\mathbf{A})$, Tr $(\mathbf{A})$ and det $(\mathbf{A})$, respectively. $\mathbf{A}\succeq 0$ means $\mathbf{A}$ is a positive semidefinite (PSD) matrix. The symbol $\mathbf{I}$ denotes the identity matrix and $\mathbf{0}$ denotes a zero vector or matrix, The symbol $\mathbb{E}\{.\}$ represents the statistical expectation of the argument.

II. System Model

Consider a downlink network model for a SWIPT system as shown in Figure 1, where a N_{T}-antenna transmitter intends to transmit the RF signals to N single-antenna IRs and S N_{R}-antenna ERs. It is assumed that only the IRs are the authorized users to decode the information. Each ER is only expected to facilitate EH with the received RF signals. There are K single-antenna Eves in the system, who intend to intercept the confidential information from the RF signals between the transmitter and IRs. Considering that ERs may also be able to decode the confidential information maliciously,[2] MARSs are embedded in the transmit signals to confuse both ERs and Eves. Therefore, only IRs are able to decode the confidential information in the RF signals correctly.

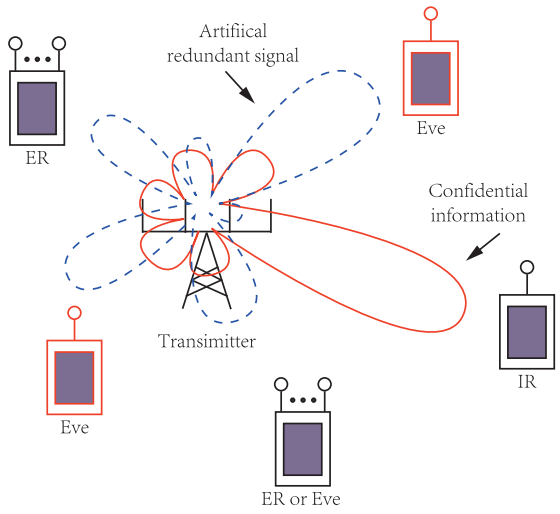

Fig. 1. System model.

For clarity, we use n, s and k to denote the n-th IR, the s-th ER and the k-th Eve, respectively, where $n\in\mathcal{N}=[1,2,\ldots,N]$, $s\in\mathcal{S}=[1,2,\ldots,S]$ and $k\in\mathcal{K}=[1,2,\ldots,K]$.

Denote $\mathbf{h}_n\in\mathbb{C}^{N_{\mathrm{T}}\times 1}$, $\mathbf{G}_s\in\mathbb{C}^{N_{\mathrm{T}}\times N_{\mathrm{R}}}$ and $\mathbf{g}_k\in\mathbb{C}^{N_{\mathrm{T}}\times 1}$ to be the channel coefficient vectors of the n-th IR, the s-th ER and the k-th Eve[3] from the transmitter, respectively. In the perfect CSI case, it is assumed that no channel errors are involved in the CSI estimation and feedback. Thus, beamforming vectors can be generated accurately to concentrate over the directions of the IRs, and the energy-bearing MARSs can be also accurately generated to concentrate over the directions of the ERs and the Eves. Owing to perfect CSI, the theoretical minimum power is needed to meet the QoS and secure requirements. So this case is often used to explore the system potential performance limit and the corresponding transmit design is referred to *non-robust design*.

Nevertheless, in practice, due to the channel fading, signal interference, high mobility, limited computational capacity and limited feedback channel, some errors may be involved in the CSI feedback, referring to imperfect CSI case, where both the beamforming vectors and the MARSs cannot be generated accurately anymore. In this case, the channels of n-th IR, s-th

[1] So far, no work has been done for our considered system even in the case of single ARS or in the case of traditional linear EH model.

[2] Although the circuits for EH and ID are different, compared to IRs, ERs are often deployed closer to the transmitter, since ERs need to operate with significantly higher received power. That is, ERs have relatively good channel conditions than IRs. In this case, once ERs employ information decoding circuits, it is of very high probability for them to eavesdrop the information transmitted to IRs. This is with a great potential to threaten the secrecy of the system. In order to guarantee a more stringent information security, similar to [23] and [24], we also assume that ERs may have the ability to decode the information and eavesdrop IRs.

[3] The CSI of Eve can be estimated at the transmitter through the local oscillator power inadvertently leaked from the Eve's receiver RF frontend [33].

ER and k-th Eve are described by

$$\mathbf{h}_n = \hat{\mathbf{h}}_n + \mathbf{e}_n^{(\mathrm{IR})} \in \mathbb{C}^{N_\mathrm{T}\times 1}, \tag{1}$$

$$\mathbf{G}_s = \hat{\mathbf{G}}_s + \mathbf{E}_s \in \mathbb{C}^{N_\mathrm{T}\times N_\mathrm{R}}, \tag{2}$$

and

$$\mathbf{g}_k = \hat{\mathbf{g}}_k + \mathbf{e}_k^{(\mathrm{Eve})} \in \mathbb{C}^{N_\mathrm{T}\times 1}, \tag{3}$$

where $\hat{\mathbf{h}}_n$, $\hat{\mathbf{g}}_k \in \mathbb{C}^{N_\mathrm{T}\times 1}$ and $\hat{\mathbf{G}}_s \in \mathbb{C}^{N_\mathrm{T}\times N_\mathrm{R}}$ denote the available channel estimates at the transmitter, and $\mathbf{e}_n^{\mathrm{IR}}$, $\mathbf{e}_k^{\mathrm{Eve}} \in \mathbb{C}^{N_\mathrm{T}\times 1}$ and $\mathbf{E}_s \in \mathbb{C}^{N_\mathrm{T}\times N_\mathrm{R}}$ denote the channel errors, which are assumed to be deterministic and bounded, such as

$$\left\|\mathbf{e}_n^{(\mathrm{IR})}\right\|_2^2 \le \varepsilon_n^{(\mathrm{IR})}, \quad \left\|\mathbf{E}_s\right\|_\mathrm{F}^2 \le \varepsilon_s^{(\mathrm{ER})}, \quad \left\|\mathbf{e}_k^{(\mathrm{Eve})}\right\|_2^2 \le \varepsilon_k^{(\mathrm{Eve})},$$

with $\varepsilon_n^{(\mathrm{IR})}$, $\varepsilon_s^{(\mathrm{ER})}$, $\varepsilon_k^{(\mathrm{Eve})} \ge 0$ denoting the sizes of the errors and the corresponding transmit design is referred to *the robust design*. In this paper, both the non-robust and the robust designs are investigated.

Let $\vartheta_n(t) \in \mathbb{C}$ denote the desired symbol of the n-th IR, and without loss of generality, it is assumed that $\mathbb{E}\left\{|\vartheta_n(t)|^2\right\} = 1$. In each time slot, the transmit signal by the transmitter in both the perfect CSI case and the imperfect CSI case can be uniformly given by

$$\mathbf{x}(t) = \sum\nolimits_{n=1}^{N} \mathbf{w}_n \vartheta_n(t) + \sum\nolimits_{l=1}^{L} \mathbf{z}_l(t) \in \mathbb{C}^{N_\mathrm{t}\times 1}, \tag{4}$$

where $\mathbf{w}_n \in \mathbb{C}^{N_\mathrm{T}\times 1}$ is the relevant beamforming vector. $l \in \mathcal{L} = [1, 2, \ldots, L]$ and L is the number of MARSs. $\mathbf{z}_l(t) \in \mathbb{C}^{N_\mathrm{T}\times 1}$ indicates the l-th energy-bearing MARS with Gaussian distribution, i.e., $\mathbf{z}_l(t) \sim \mathcal{CN}(\mathbf{0}, \Sigma_l)$ with $\Sigma_l \succeq \mathbf{0}$. Then, the total transmit power of the transmitter is

$$\sum\nolimits_{n=1}^{N} \|\mathbf{w}_n\|_2^2 + \sum\nolimits_{l=1}^{L} \mathrm{Tr}(\Sigma_l).$$

The received signals at the n-th IR, s-th ER and k-th Eve can be given respectively by

$$y_n^{(\mathrm{IR})} = \sum_{n=1}^{N} \mathbf{h}_n^H \mathbf{w}_n \vartheta_n(t) + \sum_{l=1}^{L} \mathbf{h}_n{}^H \mathbf{z}_l(t) + n_n^{(\mathrm{IR})}(t), \tag{5}$$

$$\mathbf{y}_s^{(\mathrm{ER})} = \sum_{n=1}^{N} \mathbf{G}_s^H \mathbf{w}_n \vartheta_n(t) + \sum_{l=1}^{L} \mathbf{G}_s^H \mathbf{z}_l(t) + \mathbf{n}_s^{(\mathrm{ER})}(t), \tag{6}$$

and

$$y_k^{(\mathrm{Eve})} = \sum_{n=1}^{N} \mathbf{g}_k^H \mathbf{w}_n \vartheta_n(t) + \sum_{l=1}^{L} \mathbf{g}_k^H \mathbf{z}_l(t) + n_k^{(\mathrm{Eve})}(t), \tag{7}$$

where $n_n^{(\mathrm{IR})}(t) \sim \mathcal{CN}(0, \sigma^2)$, $\mathbf{n}_s^{(\mathrm{ER})}(t) \sim \mathcal{CN}(0, \sigma^2\mathbf{I}_{N_\mathrm{R}})$ and $n_k^{(\mathrm{Eve})}(t) \sim \mathcal{CN}(0, \sigma^2)$ are the additive white Gaussian noises (AWGN) at the n-th IR, s-th ER and k-th Eve, respectively, with σ^2 denoting the noise power at the each receiver.

Both the IRs and the Eves intend to decode the information with their received RF signals. Thus, following (5) and (7), the received SINR at the n-th IR and the k-th Eve can be expressed by (8) and (9), as shown at the bottom of this page, respectively. The ERs may be able to decode the information with their received signals, where the received SINR at the s-th ER can be given by (10), as shown at the bottom of this page, in terms of (6). Note that the max terms in (9) and (10) indicate the maximum received SINR associated with the N IRs at the Eve or ER should be lower than a pre-given threshold. In our considered system, to guarantee the information security, we do not allow any IR to be eavesdropped by any Eve or ER. Thus, we consider the worst case. If the maximum received SINR associated with the N IRs at the Eve or ER should be lower than a pre-given threshold, no IR will be eavesdropped.

The ERs harvest energy from the received RF signals, where the power carried in the received RF signals is converted into DC currency by RF-EH circuits. The input power (i.e., the power carried in the received RF signals) at the s-th ER is

$$P_s^{(\mathrm{ER})}\left(\{\mathbf{w}_n,\}_{n=1}^N, \{\Sigma_l\}_{l=1}^L\right) = \mathrm{Tr}\left(\mathbf{G}_s^H\left(\sum\nolimits_{n=1}^{N}\mathbf{w}_n\mathbf{w}_n^H + \sum\nolimits_{l=1}^{L}\Sigma_l\right)\mathbf{G}_s\right).$$

For RF-EH circuits, one of the most important parameters is the RF-to-DC conversion efficiency η, which is demonstrated by the ratio of the output DC power to the input RF power. In most existing works [23], [25]–[32], η was regarded as a constant that takes the value in the interval $(0, 1]$. That is, the harvested energy at the s-th ER $\Phi_s = \eta P_s^{(\mathrm{ER})}$, referring to *the linear EH model*, which means that the RF-to-DC conversion efficiency η is independent of the input power level. However, in practice, the RF-EH circuits include various non-linearities, such as the diode or diode-connected transistor. Thus, the RF-to-DC conversion efficiency depends on the input power level. To capture the dynamics of the RF-to-DC conversion efficiency for different input power levels, the non-linear EH model presented in [8] and [9] is adopted in this paper. Thus, the output DC power (i.e., the harvested power)

$$\mathrm{SINR}_n^{(\mathrm{IR})}\left(\{\mathbf{w}_n,\}_{n=1}^N, \{\Sigma_l\}_{l=1}^L\right) = \frac{\left|\mathbf{h}_n^H\mathbf{w}_n\right|^2}{\sum_{m\ne n}^{N}\left|\mathbf{h}_n^H\mathbf{w}_m\right|^2 + \sum_{l=1}^{L}\mathbf{h}_n^H\Sigma_l\mathbf{h}_n + \sigma^2} \tag{8}$$

$$\mathrm{SINR}_k^{(\mathrm{Eve})}\left(\{\mathbf{w}_n,\}_{n=1}^N, \{\Sigma_l\}_{l=1}^L\right) = \max_{n\in\mathcal{N}}\left\{\frac{\left|\mathbf{g}_k^H\mathbf{w}_n\right|^2}{\sum_{m\ne n}^{N}\left|\mathbf{g}_k^H\mathbf{w}_m\right|^2 + \sum_{l=1}^{L}\mathbf{g}_k^H\Sigma_l\mathbf{g}_k + \sigma^2}\right\} \tag{9}$$

$$\mathrm{SINR}_s^{(\mathrm{ER})}\left(\{\mathbf{w}_n,\}_{n=1}^N, \{\Sigma_l\}_{l=1}^L\right) = \max_{n\in\mathcal{N}}\left\{\det\left(\mathbf{I} + \left(\sum_{m\ne n}^{N}\mathbf{G}_s^H\mathbf{w}_m\mathbf{w}_m^H\mathbf{G}_s + \sum_{l=1}^{L}\mathbf{G}_s^H\Sigma_l\mathbf{G}_s + \sigma^2\mathbf{I}\right)^{-1}\mathbf{G}_s^H\mathbf{w}_n\mathbf{w}_n^H\mathbf{G}_s\right)\right\} \tag{10}$$

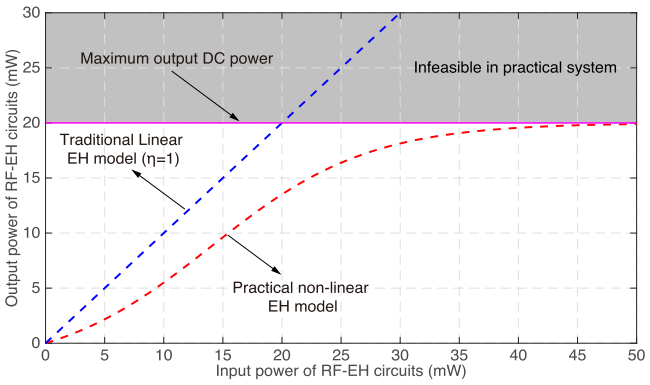

Fig. 2. Non-linear EH model where M_s is set as 20mW.

of the RF-EH circuits at the s-th ER is

$$\Phi_s\left(\{\mathbf{w}_n\}_{n=1}^N,\{\Sigma_l\}_{l=1}^L\right)=\frac{\Psi_s}{X_s}-Y_s \tag{11}$$

with

$$\Psi_s=\frac{M_s}{1+\exp\left(-a_s\left(P_s^{(\mathrm{ER})}\left(\{\mathbf{w}_n,\}_{n=1}^N,\{\Sigma_l\}_{l=1}^L\right)-b_s\right)\right)},$$

where $X_s=\frac{\exp(a_sb_s)}{1+\exp(a_sb_s)}$ and $Y_s=\frac{M_s}{\exp(a_sb_s)}$.

Ψ_s is a logistic function of $P_s^{\mathrm{ER}}\left(\{\mathbf{w}_n,\}_{n=1}^N,\{\Sigma_l\}_{l=1}^L\right)$, and M_s is a constant denoting the maximum output DC power, which indicates the saturation limitation of the RF-EH circuits. a_s and b_s are constants representing some properties of the EH system, e.g., the resistance, the capacitance and the circuit sensitivity. In general, M_s, a_s and b_s depend on the choice of hardware components for assembling the EH system and can be estimated through a standard curve fitting algorithm [8].

Figure 2 provides an example of the non-linear EH model, where the maximum output DC power M_s is set as 20mW. One can observe that the output DC power increases with the increment of the input power at first, and then when it reaches the saturation region. The output DC power cannot surpass this saturation limitation, which is much different from traditional linear EH model, where the output DC power can be always increased with the increment of the input power.

III. MARS-Aided Transmit Beamforming Design

A. Problem Formulation

The proposed design is to minimize the required power by jointly optimizing the transmit beamforming vectors $\{\mathbf{w}_n\}_{n=1}^N$ and covariance matrixes of the MARSs $\{\Sigma_l\}_{l=1}^L$ to meet the following system requirements.

- For IRs, the received SINR at the n-th IR should be larger than a predefined threshold γ_n in order to guarantee its required quality of service (QoS).
- For ERs, the harvested power at the s-th ER should be larger than a predefined threshold ς_s to meet its EH requirement. Besides, in order to prevent ERs decoding information, the added MARSs should guarantee that the s-th ER cannot decode the information accurately, i.e., the received SINR being lower than a predefined secure threshold ω_s.
- For the Eves, the added MARSs should also guarantee the received SINR at the k-th Eve lower than ϕ_k.

Then, the considered problem is mathematically expressed by[4]

$$\mathbf{P_0}:$$

$$\min_{\{\mathbf{w}_n\}_{n=1}^N,\{\Sigma_l\}_{l=1}^L}\sum_{n=1}^N\|\mathbf{w}_n\|_2^2+\sum_{l=1}^L\mathrm{Tr}\left(\Sigma_l\right) \tag{12a}$$

$$\text{s.t. } \mathrm{SINR}_n^{(\mathrm{IR})}\left(\{\mathbf{w}_n,\}_{n=1}^N,\{\Sigma_l\}_{l=1}^L\right)\geq\gamma_n \tag{12b}$$

$$\Phi_s\left(\{\mathbf{w}_n,\}_{n=1}^N,\{\Sigma_l\}_{l=1}^L\right)\geq\varsigma_s \tag{12c}$$

$$\mathrm{SINR}_s^{(\mathrm{ER})}\left(\{\mathbf{w}_n,\}_{n=1}^N,\{\Sigma_l\}_{l=1}^L\right)\leq\omega_s \tag{12d}$$

$$\mathrm{SINR}_k^{(\mathrm{Eve})}\left(\{\mathbf{w}_n,\}_{n=1}^N,\{\Sigma_l\}_{l=1}^L\right)\leq\phi_k \tag{12e}$$

$$\Sigma_l\succeq\mathbf{0},\quad\forall n\in\mathcal{N},\ \forall s\in\mathcal{S},\ \forall k\in\mathcal{K},\ l\in\mathcal{L}. \tag{12f}$$

(12b) is the received QoS constraint of the n-th IR, (12c) is the EH constraint of the s-th ER, and (12d) and (12e) are the information leakage constraints of the s-th ER and the k-th Eve, respectively.

For both the non-robust and the robust designs, the associated optimization problem can be uniformly expressed by problem P_0. However, whether for the non-robust design or the robust design, (12) is hard to cope with due to the non-convex constraints (12b)-(12e). To get some tractable results, in the next two subsections, SDR-based optimization approaches are presented to solve the non-robust design and the robust design problems, respectively.

B. Non-Robust Design With Perfect CSI

In order to explore the system potential performance limit, perfect CSI is assumed to be obtained at the transmitter and the corresponding non-robust design is investigated in this subsection. To solve the optimization problem associated with the non-robust design, we first deal with the non-convex constraints as follows.

For the received QoS constraint (12b), it can be exactly rewritten as

$$\frac{1}{\gamma_n}\left|\mathbf{h}_n^H\mathbf{w}_n\right|^2\geq\sum_{m\neq n}^N\left|\mathbf{h}_n^H\mathbf{w}_m\right|^2+\sum_{l=1}^L\mathbf{h}_n^H\Sigma_l\mathbf{h}_n+\sigma^2. \tag{13}$$

(13) is non-convex due to the quadratic terms of $\mathbf{w}_n$ in both sides. By defining $\mathbf{W}_n=\mathbf{w}_n\mathbf{w}_n^H$ with $\mathbf{W}_n\succeq\mathbf{0}$ and $\mathrm{Rank}\left(\mathbf{W}_n\right)=1$, (13) can be equivalently transformed to be

$$\mathrm{Tr}\left(\mathbf{h}_n\mathbf{h}_n^H\left(\frac{1}{\gamma_n}\mathbf{W}_n-\sum_{m\neq n}^N\mathbf{W}_m-\sum_{l=1}^L\Sigma_l\right)\right)\geq\sigma^2. \tag{14}$$

[4]We unify the problem formulation for both the non-robust and robust designs as the non-robust design can be regarded as a special case of the robust one by setting all channel errors as zero. However, this is by no means that both problems can be efficiently solved by using a same solving approach. Therefore, we design the solving approaches for them separately.

Similarly, the information leakage constraint (12e) can also be equivalently transformed to be

$$\mathrm{Tr}\left(\mathbf{g}_k\mathbf{g}_k^H\left(\frac{1}{\phi_k}\mathbf{W}_n-\sum_{m\neq n}^{N}\mathbf{W}_m-\sum_{l=1}^{L}\Sigma_l\right)\right)\leq\sigma^2. \quad (15)$$

For the EH constraint (12c), it can be represented by

$$\mathrm{Tr}\left(\mathbf{G}_s^H\left(\sum\nolimits_{n=1}^{N}\mathbf{w}_n{\mathbf{w}_n}^H+\sum\nolimits_{l=1}^{L}\Sigma_l\right)\mathbf{G}_s\right)\geq\partial_s, \quad (16)$$

where $\partial_s=b_s-\frac{\ln\left(\frac{M_s}{X_s(\varsigma_s+Y_s)}-1\right)}{a_s}$, which is determined by the EH system and the system requirement. Also, with the definition of $\mathbf{W}_n$, (16) can be equivalently re-expressed as

$$\mathrm{Tr}\left(\mathbf{G}_s^H\left(\sum\nolimits_{n=1}^{N}\mathbf{W}_n+\sum\nolimits_{l=1}^{L}\Sigma_l\right)\mathbf{G}_s\right)\geq\partial_s. \quad (17)$$

The information leakage constraint (12d) is also non-convex and the determinant term makes it intractable. To cope with (12d), the Proposition 1 is presented. Before that we address the following Lemma 1 at first.

Lemma 1 [20]: For $\mathbf{A}\succeq\mathbf{0}$*, it holds that* $\det(\mathbf{I}+\mathbf{A})\geq 1+\mathrm{Tr}(\mathbf{A})$*, and the equality holds if and only if* $\mathrm{Rank}(\mathbf{A})\leq 1$.

Proof: The proof of Lemma 1 can be seen in Appendix A. ■

Proposition 1: The information leakage constraint (12d) is equivalent to the following inequality (18) for $\forall n\in\mathcal{N}$.

$$\mathrm{Tr}\left(\mathbf{G}_s^H\mathbf{w}_n\mathbf{w}_n^H\mathbf{G}_s\right)-(\omega_s-1)\,\mathrm{Tr}\left(\mathbf{G}_s^H\left(\sum_{m\neq n}^{N}\mathbf{w}_n\mathbf{w}_n^H+\sum_{l\neq 1}^{L}\Sigma_l\right)\mathbf{G}_s+\sigma^2\mathbf{I}\right)\leq 0. \quad (18)$$

Proof: Let

$$\mathbf{U}_s=\left(\sum_{m\neq n}^{N}\mathbf{G}_s^H\mathbf{w}_m\mathbf{w}_m^H\mathbf{G}_s+\sum_{l=1}^{L}\mathbf{G}_s^H\Sigma_l\mathbf{G}_s+\sigma^2\mathbf{I}\right)^{-1}.$$

Since $\mathbf{G}_s\succ\mathbf{0}$ and $\mathbf{I}$ is full-rank, $\mathbf{U}_s$ is full-rank and invertible. Moreover, we can have that $\mathrm{Rank}\left(\mathbf{U}_s\left(\mathbf{G}_s^H\mathbf{w}_n{\mathbf{w}_n}^H\mathbf{G}_s\right)\right)\leq 1$, because $\mathrm{Rank}\left(\mathbf{w}_n\mathbf{w}_n^H\right)=1$ and

$$\mathrm{Rank}\left(\mathbf{U}_s\left(\mathbf{G}_s^H\mathbf{w}_n\mathbf{w}_n^H\mathbf{G}_s\right)\right)\leq \min\left\{\mathrm{Rank}(\mathbf{U}_s),\mathrm{Rank}\left(\mathbf{w}_n\mathbf{w}_n^H\right),\mathrm{Rank}(\mathbf{G}_s)\right\}.$$

Then, according to Lemma 1, we have

$$\det\left(\mathbf{I}+\left(\mathbf{U}_s\left(\mathbf{G}_s^H\mathbf{w}_n{\mathbf{w}_n}^H\mathbf{G}_s\right)\right)\right)=1+\mathrm{Tr}\left(\mathbf{U}_s\left(\mathbf{G}_s^H\mathbf{w}_n{\mathbf{w}_n}^H\mathbf{G}_s\right)\right). \quad (19)$$

Following (19), (12d) can be expressed as

$$\max_{n\in\mathcal{N}}\left\{\mathrm{Tr}\left(\mathbf{U}_s\mathbf{G}_s^H\mathbf{w}_n{\mathbf{w}_n}^H\mathbf{G}_s\right)\right\}\leq\omega_s-1$$

which means that

$$\max_{n\in\mathcal{N}}\lambda_{\max}\left\{\left(\mathbf{U}_s\left(\mathbf{G}_s^H\mathbf{w}_n{\mathbf{w}_n}^H\mathbf{G}_s\right)\right)\right\}\leq\omega_s-1. \quad (20)$$

As proved previously, $\mathbf{U}_s$ is an invertible matrix, (20) can be equivalently expressed by

$$\left(\mathbf{G}_s^H\mathbf{w}_n{\mathbf{w}_n}^H\mathbf{G}_s\right)\preceq(\omega_s-1)\,\mathbf{U}_s^{-1},\quad\text{for } n\in\mathcal{N}. \quad (21)$$

That is, (18) holds and proposition 1 is proved. ■

Corollary 1: The relaxed problem with constraint (18) has the same solution with the primal problem with constraint (12b).

Proof: As shown in (19), the left-hand side of (12b) is equivalently transformed to the right-hand side of (19). That is, by substituting (12b) with (18), the feasible set does not change, so the optimal solution and result keep unchanged. ■

With the definition of $\mathbf{W}_n$, (18) is further equivalently expressed as

$$\mathrm{Tr}\left(\mathbf{G}_s^H\mathbf{W}_n\mathbf{G}_s\right)-(\omega_s-1)\times\mathrm{Tr}\left(\mathbf{G}_s^H\left(\sum_{m\neq n}^{N}\mathbf{W}_m+\sum_{l\neq 1}^{L}\Sigma_l\right)\mathbf{G}_s+\sigma^2\mathbf{I}\right)\leq 0. \quad (22)$$

By doing so, (12d) is transformed into (22), which is tractable. Thus, we replace (22) with (12d) to solve the optimization problem associated with the non-robust design. Further, by replacing the constraints (12b)-(12e) with (14), (15), (17), (22), problem P_0 is transformed into the following problem P_1

$$\begin{aligned}\mathbf{P_1}:\ &\min_{\{\mathbf{W}_n\}_{n=1}^{N},\{\Sigma_l\}_{l=1}^{L}}\ \sum\nolimits_{n=1}^{N}\mathrm{Tr}(\mathbf{W}_n)+\sum\nolimits_{l=1}^{L}\mathrm{Tr}(\Sigma_l)\\ &\text{s.t. (14), (15), (17), (22),}\quad \mathbf{W}_n\succeq\mathbf{0},\\ &\qquad\mathrm{Rank}(\mathbf{W}_n)=1,\quad \Sigma_l\succeq\mathbf{0},\ \forall n\in\mathcal{N},\\ &\qquad\forall s\in\mathcal{S},\quad\forall k\in\mathcal{K},\ l\in\mathcal{L}. \end{aligned} \quad (23)$$

Although the objective function and all constraints in problem P_1 are computational tractable, it is still non-convex due to the rank-one constraint, i.e., $\mathrm{Rank}(\mathbf{W}_n)=1$. With SDR, by dropping the rank-one constraint, we obtain its SDR form as

$$\begin{aligned}\mathbf{P_{1-A}}:\ &\min_{\{\mathbf{W}_n\}_{n=1}^{N},\{\Sigma_l\}_{l=1}^{L}}\ \sum\nolimits_{n=1}^{N}\mathrm{Tr}(\mathbf{W}_n)+\sum\nolimits_{l=1}^{L}\mathrm{Tr}(\Sigma_l)\\ &\text{s.t. (14), (15), (17), (22),}\quad \mathbf{W}_n\succeq\mathbf{0},\\ &\qquad\Sigma_l\succeq\mathbf{0},\ \forall n\in\mathcal{N},\ \forall s\in\mathcal{S},\ \forall k\in\mathcal{K},\ l\in\mathcal{L}. \end{aligned} \quad (24)$$

$\mathrm{P}_{1-\mathrm{A}}$ is a convex optimization problem, whose optimal solution $\left\{\mathbf{W}_n^\star,\Sigma_n^\star\right\}$ can be obtained by using some convex optimization solving approaches. The goal of the original problem P_0 is to find the optimal $\left\{\mathbf{w}_n^\star\right\}$ rather than $\left\{\mathbf{W}_n^\star\right\}$. It is worthy to note that only when the rank of $\mathbf{W}_n^\star$ is 1, the global optimal $\left\{\mathbf{w}_n^\star\right\}$ can be recovered.

Proposition 2: The rank-one solution to problem $\mathrm{P}_{1-\mathrm{A}}$ *always exists in the perfect CSI case.*

Proof: The proof of proposition 2 can be seen in Appendix B. ■

With proposition 2, the optimal $\mathbf{w}_n^\star$ to the non-robust design can always be derived by rank-one decomposition of $\mathbf{W}_n^\star$.

C. Robust Design With Imperfect CSI

In practical systems, due to the channel fading, signal interference, high mobility, limited computational capacity and limited feedback channel, the perfect CSI may not always be obtained, which results in the imperfect CSI case. Therefore, the non-robust beamforming design may not always meet the system requirements. To guarantee the QoS of receivers, the robust transmit design is investigated in this subsection for our considered secure SWIPT system.

In the imperfect CSI, for the n-th IR, similar to the perfect CSI case, with the definition of $\mathbf{W}_n = \mathbf{w}_n\mathbf{w}_n^H$ with $\mathbf{W}_n \succeq \mathbf{0}$, the SDR form of its received QoS constraint (12b) can be equivalently expressed by

$$\left(\hat{\mathbf{h}}_n + \mathbf{e}_n^{(\mathrm{IR})}\right)^H \mathbf{M}_n \left(\hat{\mathbf{h}}_n + \mathbf{e}_n^{(\mathrm{IR})}\right) \geq \sigma^2, \tag{25}$$

where

$$\mathbf{M}_n = \tfrac{1}{\gamma_n}\mathbf{W}_n - \sum\nolimits_{m\neq n}^{N} \mathbf{W}_m - \sum\nolimits_{l=1}^{L} \Sigma_l.$$

For the s-th ER, the SDR forms of its EH constraint (12c) and information leakage constraint (12d) are equivalently represented by (27) and (28), as shown at the bottom of this page, respectively.

For the k-th Eve, the SDR forms of its information leakage constraint (12e) are equivalently expressed as

$$\left(\hat{\mathbf{g}}_k + \mathbf{e}_k^{(\mathrm{Eve})}\right)^H \mathbf{N}_k \left(\hat{\mathbf{g}}_k + \mathbf{e}_k^{(\mathrm{Eve})}\right) \leq \sigma^2, \tag{26}$$

where

$$\mathbf{N}_k = \tfrac{1}{\phi_k}\mathbf{W}_n - \sum\nolimits_{m\neq n}^{N} \mathbf{W}_m - \sum\nolimits_{l=1}^{L} \Sigma_l.$$

By dropping the constraint of $\mathrm{Rank}\,(\mathbf{W}_n) = 1$, the SDR form of the optimization problem associated with the robust design can be given by the following problem P_2.

$$\begin{aligned}\mathbf{P_2}: \min_{\{\mathbf{W}_n\}_{n=1}^N, \{\Sigma_l\}_{l=1}^L} & \sum_{n=1}^{N} \mathrm{Tr}\,(\mathbf{W}_n) + \sum_{l=1}^{L} \mathrm{Tr}\,(\Sigma_l) \\ \text{s.t. } & (25), (26), \ (27), \ (28), \ \left\|\mathbf{e}_n^{(\mathrm{IR})}\right\|_2^2 \leq \varepsilon_n^{(\mathrm{IR})}, \\ & \left\|\mathbf{E}_s\right\|_{\mathrm{F}}^2 \leq \varepsilon_s^{(\mathrm{ER})}, \quad \left\|\mathbf{e}_k^{(\mathrm{Eve})}\right\|_2^2 \leq \varepsilon_k^{(\mathrm{Eve})}, \\ & \mathbf{W}_n \succeq \mathbf{0}, \quad \Sigma_l \succeq \mathbf{0}, \ \forall n \in \mathcal{N}, \ \forall s \in \mathcal{S}, \\ & \forall k \in \mathcal{K}, \quad l \in \mathcal{L}. \end{aligned} \tag{29}$$

Since the objective function and all constraints in problem P_2 are linear in $\{\mathbf{W}_n, \Sigma_l\}$, it is a convex problem. However, problem P_2 is still challenging to be solved due to the infinite number of constraints induced by the channel errors. To find a tractable form for problem problem P_2, a S-procedure based solving approach is proposed, where S-procedure is used to convert the quadratic inequality into a semidefinite matrix inequality. For the readers' convenience, the detail of S-procedure is summarized briefly in Lemma 2 as follows.

Lemma 2 [34]: If $f(\mathbf{X}) = \mathbf{X}^H\mathbf{A}\mathbf{X} + \mathbf{X}^H\mathbf{B} + \mathbf{B}^H\mathbf{X} + \mathbf{C}$, *and* $\mathbf{D} \succeq \mathbf{0}$, *the following two statements are equivalent to each other:*

1) : $f(\mathbf{X}) \succeq \mathbf{0}, \quad \forall \mathbf{X} \in \left\{\mathbf{X} \middle| \mathrm{Tr}\left(\mathbf{D}\mathbf{X}\mathbf{X}^H\right) \leq 1\right\}$;

2) : $\exists t \geq 0$, such that $\begin{bmatrix} \mathbf{A} & \mathbf{B}^H \\ \mathbf{B} & \mathbf{C} \end{bmatrix} - t\begin{bmatrix} -\mathbf{D} & 0 \\ 0 & \mathbf{I} \end{bmatrix} \succeq \mathbf{0}$.

Proof: The proof of Lemma 2 can be seen in [34], which is omitted here. ■

Lemma 2 indicates that $\mathbf{X}$ in the second-order function $f(\mathbf{X})$ can be removed by introducing a positive variable t and converting $f(\mathbf{X})$ into a linear matrix inequality (LMI). Motivated by this, we remove the channel errors in (25)-(28) by introducing some positive slack variables $t_n^{(\mathrm{IR})}$, $\tau_s^{(\mathrm{ER})}$, $t_s^{(\mathrm{ER})}$ and $t_k^{(\mathrm{Eve})}$, and then, (25)-(28) are equivalently transformed to be (30), as shown at the bottom of this page, where

$$\mathbf{F} = \sum_{n=1}^{N} \mathbf{W}_n + \sum_{l=1}^{L} \Sigma_l, \ \theta_s = \frac{b_s}{N_{\mathrm{T}}} - \frac{\ln\left(\frac{M_s}{(\varsigma_s + Y_s)X_s}\right)}{a_s N_{\mathrm{T}}}$$

$$\mathrm{Tr}\left(\left(\hat{\mathbf{G}}_s + \mathbf{E}_s\right)^H \left(\sum\nolimits_{n=1}^{N} \mathbf{W}_n + \sum\nolimits_{l=1}^{L} \Sigma_l\right)\left(\hat{\mathbf{G}}_s + \mathbf{E}_s\right)\right) \geq b_s - \frac{\ln\left(\frac{M_s}{(\varsigma_s + Y_s)X_s}\right)}{a_s} \tag{27}$$

$$\left(\hat{\mathbf{G}}_s + \mathbf{E}_s\right)^H \left(\mathbf{W}_n - (\omega_s - 1)\left(\sum\nolimits_{m\neq n}^{N} \mathbf{W}_m + \sum\nolimits_{l=1}^{L} \Sigma_l\right)\right)\left(\hat{\mathbf{G}}_s + \mathbf{E}_s\right) + (\omega_s - 1)\sigma^2\mathbf{I} \preceq \mathbf{0} \tag{28}$$

$$\begin{cases} \begin{bmatrix} t_n^{(\mathrm{IR})}\mathbf{I} + \mathbf{M}_n & \mathbf{M}_n\hat{\mathbf{h}}_n \\ \hat{\mathbf{h}}_n^H\mathbf{M}_n & \hat{\mathbf{h}}_n^H\mathbf{M}_n\hat{\mathbf{h}}_n - t_n^{(\mathrm{IR})}\varepsilon_n^{(\mathrm{IR})} - \sigma^2 \end{bmatrix} \succeq \mathbf{0}, \\ \begin{bmatrix} \tau_s^{(\mathrm{ER})}\mathbf{I} + \mathbf{F} & \mathbf{F}\hat{\mathbf{G}}_s \\ \hat{\mathbf{G}}_s^H\mathbf{F} & \hat{\mathbf{G}}_s^H\mathbf{F}\hat{\mathbf{G}}_s - \left(\theta_s + \tau_s^{(\mathrm{ER})}\varepsilon_s^{(\mathrm{ER})}\right)\mathbf{I} \end{bmatrix} \succeq \mathbf{0}, \\ \begin{bmatrix} t_s^{(\mathrm{ER})}\mathbf{I} + \mathbf{T}_s & \mathbf{T}_s\hat{\mathbf{G}}_s \\ \hat{\mathbf{G}}_s^H\mathbf{T}_s & \hat{\mathbf{G}}_s^H\mathbf{T}_s\hat{\mathbf{G}}_s - \left((\omega_s - 1)\sigma^2 + t_s^{(\mathrm{ER})}\varepsilon_s^{(\mathrm{ER})}\right)\mathbf{I} \end{bmatrix} \succeq \mathbf{0}, \\ \begin{bmatrix} t_k^{(\mathrm{Eve})}\mathbf{I} - \mathbf{N}_k & -\mathbf{N}_k\hat{\mathbf{g}}_k \\ -\hat{\mathbf{g}}_k^H\mathbf{N}_k & \sigma^2 - t_k^{(\mathrm{Eve})}\varepsilon_k^{(\mathrm{Eve})} - \hat{\mathbf{g}}_k^H\mathbf{N}_k\hat{\mathbf{g}}_k \end{bmatrix} \succeq \mathbf{0}. \end{cases} \tag{30}$$

TABLE I
COMPUTATIONAL ANALYSIS

Design	Complexity order
Non-robust design	$\sqrt{2N_{\mathrm{T}}\left(N\left(K+S+1\right)+S\right)}\ln\left(1/\varepsilon\right)\left(\left(N\left(K+S+1\right)+S\right)\left(\tilde{n}N_{\mathrm{T}}+\tilde{n}^2{N_{\mathrm{T}}}^2\right)+\tilde{n}^3\right)$
Robust design	$2\sqrt{N_{\mathrm{T}}S\left(N+1\right)}\ln\left(1/\varepsilon\right)\left(\tilde{n}N\left(K+1\right)\left(N_{\mathrm{T}}+1\right)\right.$ $\left.+2\tilde{n}S\left(N+1\right)N_{\mathrm{T}}+4\tilde{n}S\left(N+1\right){N_{\mathrm{T}}}^2+\tilde{n}^2N\left(K+1\right)\left(N_{\mathrm{T}}+1\right)^2+2\tilde{n}^3\right)$

and

$$\mathbf{T}_s=\left(\omega_s-1\right)\left(\sum\nolimits_{m\neq n}^{N}\mathbf{W}_m+\sum\nolimits_{l=1}^{L}\Sigma_l\right)-\mathbf{W}_n.$$

Since the inequalities in (30) are all LMIs, they construct a convex set of all variables, i.e., $\left\{\mathbf{W}_n,\boldsymbol{\Sigma}_l,t_n^{(\mathrm{IR})},\tau_s^{(\mathrm{ER})},t_s^{(\mathrm{ER})},t_k^{(\mathrm{Eve})}\right\}$. More importantly, the number of constraints in (30) is finite. That is, the infinite number of constraints in problem P_2 are equivalently transformed into finite ones in (30), which makes problem P_2 computational trackable. As a result, problem P_2 is equivalently transformed into the following problem $\mathrm{P}_{2-\mathrm{A}}$.

$$\begin{aligned}\mathbf{P_{2-A}}:\ &\min_{\left\{\substack{\mathbf{W}_n,\boldsymbol{\Sigma}_l,t_n^{(\mathrm{IR})},\\ \tau_s^{(\mathrm{ER})},t_s^{(\mathrm{ER})},t_k^{(\mathrm{Eve})}}\right\}}\ \sum_{n=1}^{N}\mathrm{Tr}\left(\mathbf{W}_n\right)+\sum_{l=1}^{L}\mathrm{Tr}\left(\Sigma_l\right)\\ &\text{s.t. (30)},\quad \mathbf{W}_n\succeq\mathbf{0},\ \Sigma_l\succeq\mathbf{0},\ t_n^{(\mathrm{IR})}\geq 0,\\ &\quad \tau_s^{(\mathrm{ER})}\geq 0,\quad t_s^{(\mathrm{ER})}\geq 0,\ t_k^{(\mathrm{Eve})}\geq 0,\\ &\quad \forall n\in\mathcal{N},\quad \forall s\in\mathcal{S},\ \forall k\in\mathcal{K},\ l\in\mathcal{L}.\end{aligned}\tag{31}$$

Therefore, problem $\mathrm{P}_{2-\mathrm{A}}$ can be solved by using standard convex optimization solvers, e.g., SeduMi or CVX [35]. That is, the optimal $\{\mathbf{W}_n^\star,\Sigma_l^\star\}$ of problem $\mathrm{P}_{2-\mathrm{A}}$ is able to be derived. Note that the goal of the proposed robust design is to find the optimal $\{\mathbf{w}_n^\star\}$ rather than $\{\mathbf{W}_n^\star\}$. Thus, once we get $\{\mathbf{W}_n^\star\}$, we have to recover the corresponding $\{\mathbf{w}_n^\star\}$. If Rank $\left(\mathbf{W}_n^\star\right)=1$, $\mathbf{w}_n^\star$ can be derived by rank-one decomposition of $\mathbf{W}_n^\star$. Otherwise, if Rank $\left(\mathbf{W}_n^\star\right)>1$,[5] $\mathbf{w}_n^\star$ can be approximately derived by Gaussian randomization procedure [36], where random vectors with Gaussian distribution of covariance matrix $\mathbf{W}_n^\star$ are generated and the optimal one is selected to approximate $\mathbf{w}_n^\star$. The detailed process can be referred to [36].

In order to check the rank-one ration of the robust design, 10000 channel realizations are simulated and over 92% cases are with the rank-one $\left\{\mathbf{W}_n^\star\right\}$. This indicates that the global optimal robust design can be achieved with a high probability. For the rest cases, the approximated optimal solution can be obtained by the aforementioned Gaussian randomization procedure.

D. Complexity Analysis

Section III-B and III-C present the solving approaches for the non-robust design (i.e., Problem $\mathrm{P}_{1-\mathrm{A}}$) and the robust design (i.e., Problem $\mathrm{P}_{2-\mathrm{A}}$), respectively. This subsection shall discuss their computational complexities.

In Problem $\mathrm{P}_{1-\mathrm{A}}$ and Problem $\mathrm{P}_{2-\mathrm{A}}$, the constraints are all LMI constrains, which can be solved by using the standard interior-point method (IPM). Before giving the computational complexity, let us first review the basic elements in the complexity analysis of IPMs.

Consider the following optimization problem:

$$\begin{aligned}\mathbf{P_a}:\ &\min_{\mathbf{x}}\ \mathbf{c}^{\mathrm{T}}\mathbf{x}\\ &\text{s.t.}\ \sum\nolimits_{i=1}^{\tilde{n}}x_i\mathbf{A}_i^j-\mathbf{B}^j\in\mathbb{H}_+^{k_j}\quad\text{for } j=1,\ldots,p,\end{aligned}$$

where $\mathbf{x}=[x_1,x_2,\ldots,x_{\tilde{n}}]\in\mathbb{C}^{\tilde{n}}$ is the unknown variable vector and $\mathbf{A}_i^j,\mathbf{B}^j\in\mathbb{H}_+^{k_j}$. A generic IPM for solving Problem $\mathrm{P_a}$ includes two parts, i.e., the iteration part and the per-iteration part.

In the iteration part, the number of iterations to calculate the ε-optimal solution is on the order of $\sqrt{\sum_{j=1}^{p}2k_j}\ln\left(1/\varepsilon\right)$. In the per-iteration part, for each iteration, a search direction is found by solving a system of n linear equations with n unknown variables, which is on the order of $\tilde{n}\sum_{j=1}^{p}k_j+\tilde{n}^2\sum_{j=1}^{p}k_j^2+\tilde{n}^3$. Hence, the computational complexity of a generic IPM for solving Problem $\mathrm{P_a}$ is about

$$\sqrt{\sum\nolimits_{j=1}^{p}2k_j}\ln\left(1/\varepsilon\right)\left(\tilde{n}\sum\nolimits_{j=1}^{p}k_j+\tilde{n}^2\sum\nolimits_{j=1}^{p}k_j^2+\tilde{n}^3\right).$$

In Problem $\mathrm{P}_{1-\mathrm{A}}$, there are $N\left(K+S+1\right)+S$ LMI constraints of size N_{T}. Thus, the computational complexity order of a generic IPM for solving Problem $\mathrm{P}_{1-\mathrm{A}}$ is represented on the first row of Table I, where n is the decision variable which is on the order of $\left(N+L\right){N_{\mathrm{T}}}^2$ (i.e., $\tilde{n}\simeq\mathcal{O}\left(\left(N+L\right)N_{\mathrm{T}}^2\right)$).

In Problem $\mathrm{P}_{2-\mathrm{A}}$, there are $\left(N\left(K+1\right)\right)$ LMI constraints with size of $N_{\mathrm{T}}+1$ and $\left(S\left(N+1\right)\right)$ LMI constraints with size of $2N_{\mathrm{T}}$. Thus, the complexity order of a generic IPM for solving Problem $\mathrm{P}_{1-\mathrm{A}}$ is represented on the second row of Table I.

It is observed that the solving approach for the robust design is too complex in solving the non-robust design, and the solving approach for the non-robust design cannot solve the robust design problem. Therefore, it is essential to develop different solving approaches for different cases.

IV. DISCUSSION OF THE EFFECT OF MARSs

It is known that without AN, beamforming vectors also may be generated to meet the QoS and secure requirements for various systems [19]. Comparably, when AN is employed, the required power can be greatly reduced, which was shown via simulations in the literature [20], [21]. However, the effect

[5]Since Rank $\left(\mathbf{W}_n^\star\right)=0$ indicates $\mathbf{W}_n^\star=\mathbf{0}$, it will not be an optimal solution to problem P_2.

of AN has not been discussed theoretically, let alone the effects of MARSs. In order to get more deep insights of MARSs, in this section, we shall discuss the effect of MARSs theoretically.

Proposition 3: Compared with the non-MARS aided beamforming design, MARS-aided beamforming design consumes no more transmit power to meet the same system requirements.

Proof: The non-MARS aided beamforming design can be formulated by setting the objective function of the original problem (12) as

$$\min_{\{\mathbf{w}_n\}_{n=1}^N} \sum\nolimits_{n=1}^{N} \|\mathbf{w}_n\|_2^2 \tag{32}$$

and eliminating $\{\Sigma_1, \ldots, \Sigma_L\}$ in (12b)-(12e). The non-MARS aided beamforming design also can be solved by our proposed SDR-based solving approaches in both non-robust and robust designs. One can see that the optimal solution to the non-MARS aided beamforming design is always a feasible solution to the MARS-aided beamforming design (12), which is realized by setting $\Sigma_1 = \ldots = \Sigma_L = \mathbf{0}$. So the optimal value of (12) must be smaller than that of the non-MARS aided beamforming design, which means that the MARS-aided beamforming design uses no more power than the non-MARS aided beamforming design to achieve the same system requirements. ∎

Proposition 3 indicates that by introducing MARSs to the transmit design of the multi-antenna secure system, the total required power can be reduced. Note that it holds not only in our considered system, but also in other AN/MARSs-aided secure system.

From the proof of Proposition 3, it is observed that the more numbers of MARSs, the better system performance, i.e., less transmit power to satisfy the same system requirements. However, it is impossible to employ infinite number of MARSs due to the limitation of number of transmit antenna and spatial DoF. So it is essential to discuss the effect of the number of MARSs embedded in the transmit signals on the system power requirement. To this end, we present the following two propositions.

Theorem 1: For both the non-robust design (24) and the robust design (31), if each ARS follows Gaussian distribution, i.e., $\mathbf{z}_l(t) \sim \mathcal{CN}(\mathbf{0}, \Sigma_l)$*, and all the constraints are linear w.r.t.* $\{\Sigma_l\}_{l=1}^L$*. When* $L \geq 1$*, the number of MARSs has no effect on the system performance.*

Proof: When there is one ARS $\mathbf{z}(t) \sim \mathcal{CN}(\mathbf{0}, \Sigma)$ with $\Sigma \succeq \mathbf{0}$, i.e., $L = 1$, $\mathbf{z}(t)$ can be divided into MARSs $\{\mathbf{z}_l(t)\}_{l=1}^L$ with $\mathbf{z}_l(t) = \sum_{l=1}^L \mathbf{z}_l(t)$, where $\mathbf{z}_l(t) \sim \mathcal{CN}(\mathbf{0}, \Sigma_l)$ and $\Sigma_l \succeq \mathbf{0}$. Since $\mathbf{z}$ is a zero-mean Gaussian variable, its covariance matrix Σ can be represented by the sum of covariance matrixes of $\{\mathbf{z}_l(t)\}_{l=1}^L$, i.e., $\Sigma = \sum_{l=1}^L \Sigma_l$. On the other hand, as in (24) and (31), the objective function and constraints are all linear w.r.t. Σ or $\{\Sigma_l\}_{l=1}^L$, the separation of Σ into $\{\Sigma_l\}_{l=1}^L$ or the combination of $\{\Sigma_l\}_{l=1}^L$ to Σ has no difference, i.e.

$$\sum\nolimits_{l=1}^{L} f(\Sigma_l) = f\left(\sum\nolimits_{l=1}^{L} \Sigma_l\right) = f(\Sigma),$$

where $f(\cdot) : \mathbb{C}^{N_T \times N_T} \to \mathbb{R}$ is an additive function.[6] That is, in this case, single ARS and MARSs have the same system performance. ∎

MARSs are able to employ the advantages of the redundant spatial DoF. Theorem 1 indicates that in our considered system, the advantages of the redundant spatial DoF can be fully employed by using single ARS. Consider that more MARSs may bring more computational burden in generating the transmit beamforming vectors. Following Theorem 1, for the transmit design with linear objective function and constraints, it is better to embed single ARS in the transmit signals.

Proposition 4: For the transmit design with non-linear objective function or constraints, when the number of transmit signals (including the information signals and MARSs) is no more than that of the transmit antennas, the more MARSs (following Gaussian distribution), the better system performance.

Proof: When the number of transmit signals is no more than that of the transmit antennas, for the transmit design with non-linear objective function or constraints, single ARS $\mathbf{z}(t) \sim \mathcal{CN}(\mathbf{0}, \Sigma)$ cannot be represented by MARSs $\{\mathbf{z}_l(t)\}_{l=1}^L$ without difference, i.e.

$$\sum\nolimits_{l=1}^{L} f(\Sigma_l) \neq f\left(\sum\nolimits_{l=1}^{L} \Sigma_l\right) = f(\Sigma).$$

The optimal solution to the transmit design with L ARSs is always the feasible solution to the transmit design with L' ARSs ($L' > L$), and the associated proof is similar to the proof of Proposition 3, which is omitted here. When the number of transmit signals is greater than that of the transmit antennas, the transmitter cannot provide sufficient DoF to fully design the transmit signals. Therefore, no performance gain can be achieved. ∎

Proposition 4 requires function $\sum_{l=1}^L f(\Sigma_l) < f\left(\sum_{l=1}^L \Sigma_l\right)$. When $f(\cdot)$ is convex or concave, such a condition may not be satisfied.

V. Simulation Results

In this section, some numerical simulation results are presented to show the efficiency of our proposed MARS-aided beamforming design, where the MARS-aided and the non-MARS aided beamforming designs, the non-robust and the robust transmit designs, the non-linear and the linear EH models, and the AN-aided and the MARS-aided beamforming designs are compared and discussed in the following four subsections, respectively.

The parameters used in the simulation are listed as follows. A carrier center frequency of 915 MHz is assume with a signal bandwidth of 200 kHz. The number of IRs, ERs and Eves are set as $N = 2$, $K = 2$ and $S = 1$, respectively. The number of the transmit antenna N_T is set as 6 and that of the received antenna at each ER N_R is set as 2. The number of MARSs L is set as 2. The channel realization $\mathbf{h}_n$ and $\mathbf{g}_k$ are i.i.d. Gaussian distributed. All IRs are randomly positioned

[6] Additive functions are the solutions to Cauchy's functional equation, i.e., $f(x + y) = f(x) + f(y)$

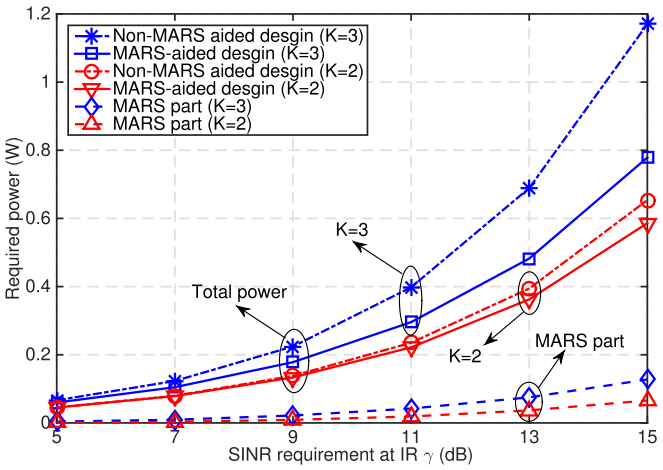

Fig. 3. Required power versus the SINR requirement at each IR where the non-MARS aided beamforming design and the MARS-aided beamforming design are compared with $K = 2$ and $K = 3$, respectively.

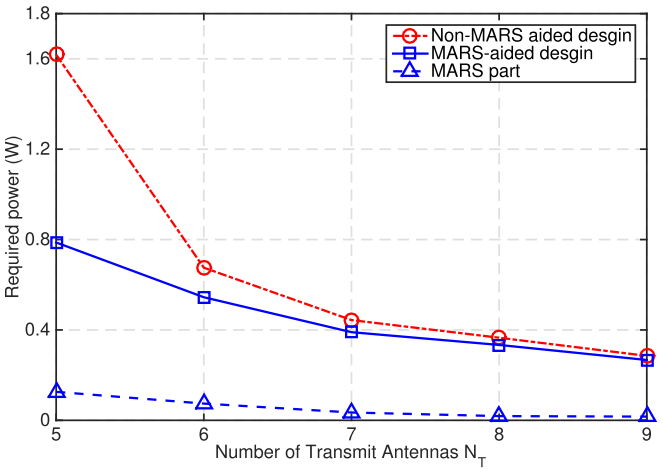

Fig. 4. Required power versus the number of transmit antennas N_{T}.

50 meters from the transmitter, which may not have line-of-sight communication channel. Therefore, the multipath fading of $\mathbf{h}_n$ between n-th ER and the transmitter is modeled as Rayleigh distribution. All ERs are randomly positioned at 10m from the transmitter, which is close enough that the line-of-sight communication channel exists. Therefore, the multipath fading of $\mathbf{G}_s$ between s-th ER and the transmitter is modeled as Rician distribution with a Rician factor of 3 dB. As for Eves, the distance between Eves and the transmitter is generated randomly within the range from 10m to 50m and the multipath fading of $\mathbf{g}_n$ between n-th Eve and the transmitter is modeled as Rayleigh distribution. We assume that all receivers' noise power is identical as $\sigma^2 = 0.05$. For simplicity, the SINR requirements at all IRs are set as the same, i.e., $\phi_k = \gamma = 10$dB. The received SINR constraints for ERs and Eves are also set the same, i.e., $\omega_s = \phi_k = 0$dB. For the robust design, the channel error radius $\varepsilon_n^{(\mathrm{IR})} = \varepsilon_s^{(\mathrm{ER})} = \varepsilon_k^{(\mathrm{Eve})} = \varepsilon = 0.01$. For the non-linear EH model, we set all M_s as 24 mW which corresponds to the maximum harvested power at each ER. Besides, we adopt $a_1 = \ldots = a_S = 150$ and $b_1 = \ldots b_S = 0.024$. The required EH power ς_s at each ER is set as 10mW. Each point in all figures is averaged over 1000 channel realizations. All parameters in the simulations are as described as above unless specified.

A. MARS-Aided vs. Non-MARS Aided Beamforming Designs

Figure 3 compares the required power of the MARS-aided and the non-MARS aided beamforming designs versus the SINR requirements at IRs, where the non-robust design is simulated. For the MARS-aided beamforming design, both the total transmit power and the MARS-part power are ploted. The simulation result demonstrates that compared with the non-MARS aided beamforming design, the proposed MARS-aided beamforming design requires much less power to satisfy the system QoS and secure requirements. The reason is that the added MARSs are able to fully utilize the spatial DoF, which is consistent with Proposition 3. It is also seen that the increment of the SINR requirement causes more total required power as well as the MARS-part power. In fact, to provide higher throughput for IRs, more power is needed in the transmit signals for the confidential information. In this case, it also becomes easier for ERs and Eves to intercept the confidential information. Therefore, more power is required in the MARSs part to cripple the interception of ERs and Eves. Figure 3 also shows the impact of the number of Eves in the system. It is observed that as the number of Eves increasing, more power is required. The reason is that for the same number of transmit antennas and DoF, when there are more Eves, the beamforming vectors are more difficult to be generate to concentrate over the direction of each IR. In this case, more power is needed to meet the system QoS and secure requirements.

The system total required power versus the number of transmit antennas is plotted in Figure 4. It can be seen that the total required power of both the MARS-aided beamforming design and the non-MARS aided beamforming design decreases with the increment of N_{T}, while the system performance gain between the MARS-aided beamforming design and the non-MARS aided beamforming design becomes smaller, because larger N_{T} yields larger spatial DoF to transmit information and energy. Moreover, it can be concluded that for the system with relatively small number of transmit antennas, MARS-aided beamforming design is a better choice to achieve lower power consumption, which is consistent with the results presented by Figure 3.

We also believe that there are some fundamental relationships between the different parameters such as N_{T}, N and L. But it is quite hard to give some explicit theoretical results on them. We tried our best to obtain some results as follows. Firstly, in our considered system, when $N_{\mathrm{T}} \geq N + L$, the transmitter has enough DoF to generate the signal beams and the AN beams. Otherwise, when $N_{\mathrm{T}} < N + L$, the signal beams and the AN beams cannot be generated, because in this case, the transmitter is overloaded. Secondly, in our considered system, since $L \geq 1$, the total required power can be reduced by employing MARSs, which is proved by Proposition 3. Thirdly, as shown in Figure 4, for our considered system, the larger difference between N_{T} and $N + L$, the less total

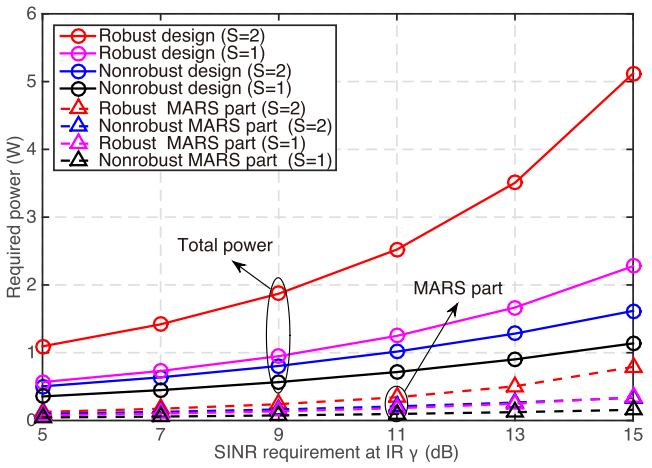

Fig. 5. Required power versus the SINR requirement at each IR where the non-robust design and the robust design are compared with $S = 1$ and $S = 2$, respectively.

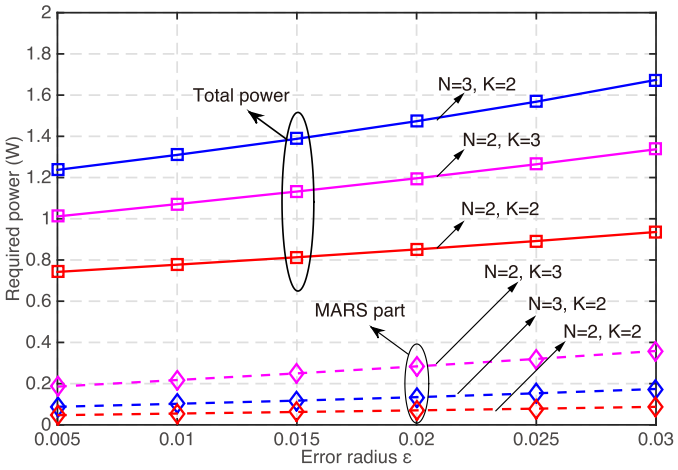

Fig. 6. Required power versus the error in the CSI feedback.

required power. Hence, to provide high-quality service to the receivers, the transmitter should be equipped with as many antennas as possible.

B. Non-Robust vs. Robust Beamforming Designs

Figure 5 compares the total required power for the non-robust design and robust design, where $N_{\mathrm{T}} = 8$. The results show that compared with the non-robust design, more transmit power is needed in the robust design. The reason is that errors involved in the CSI feedback require that the transmitter generates relatively "wider" beam to provide big enough coverage for IRs. Since in this case, it also becomes easier for ERs and Eves to intercept the information, more power is consumed in the MARSs to confuse them. As a result, the robust design consumes more power than the non-robust design. Figure 5 also indicates that the increment of ER cause more power consumption, since the transmitter is required to provide more energy to ERs as well as cripple their interception.

As for the robust beamforming design, the CSI radius error ε is a very important parameter that impacts the system performance. Figure 6 shows the result of the required power versus the CSI error radius ε. One can observe that as the

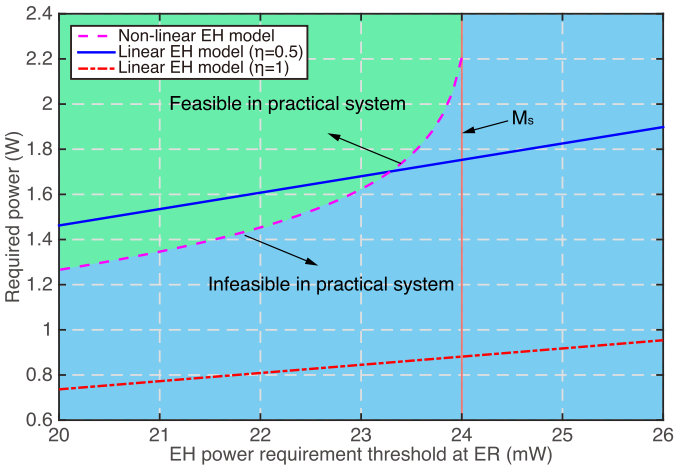

Fig. 7. Required power versus the EH power requirement at ERs under the perfect CSI assumption.

channel error radius ε increasing, more power is needed to guarantee the system QoS and secure requirement. It also can be observed that when there are more IRs in the system, more power shall be consumed, but the required power in the MARSs part change little. When there are more Eves in the system, the increment of the total required power is dominated by the increment of the required power in the MARS part. This indicates that the impact of IRs is greater than that of Eves.

C. Non-Linear vs. Linear EH Models

Figure 7 compares the non-robust design under the non-linear EH model and linear EH model, where for the linear EH model, the RF-to-DC conversion efficiency η is set as 0.5 and 1, respectively. It is observed that for the linear EH model, the total transmit power increases as the EH power requirement increases. While for the non-linear EH model, the total transmit power also increases as the EH power requirement increases, but there exists a saturation point on the EH power requirement (e.g., $M_s = 24$mW in our example) because of the non-linear RF-EH circuit feature. Moreover, if the linear EH model with $\eta = 1$ is adopted, it may result in false and deceptive output DC power. That is, when the EH power requirement is smaller than M_s, although less power is consumed by the linear EH model, the output DC power cannot meet the practical requirement (i.e., (12c) cannot be satisfied). When the EH power requirement is larger than M_s, although the transmit design can still be generated by the linear EH model, (12c) also cannot be satisfied. In contrast, for the non-linear EH model, when the EH power requirement is smaller than M_s, the EH power requirement at each ER (12c) can be guaranteed, and EH power requirement is larger than M_s, the transmit design cannot be generated because of the saturation limitation of practical RF-EH circuits. Thus, the false output DC power can be avoided by employing the non-linear EH model. Furthermore, if the linear EH model with $\eta = 0.5$ is adopted, the design under the linear EH model is also feasible in practical system but more transmit power is consumed compared with the design under the non-linear EH model. This result demonstrated the advantage of employing the non-linear EH model.

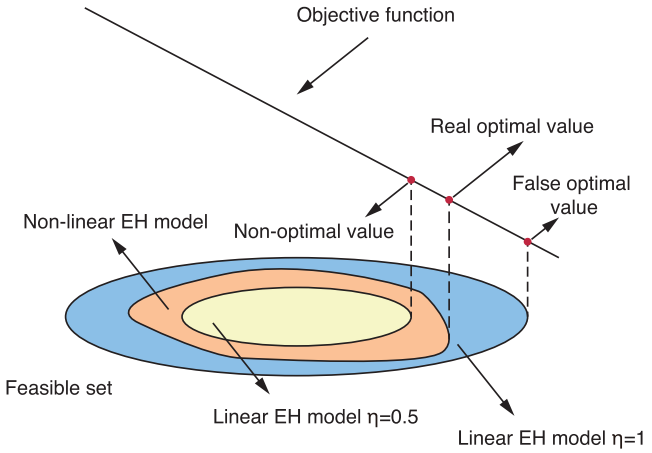

Fig. 8. Illustration of the optimal value under the Linear EH model versus the non-linear EH model.

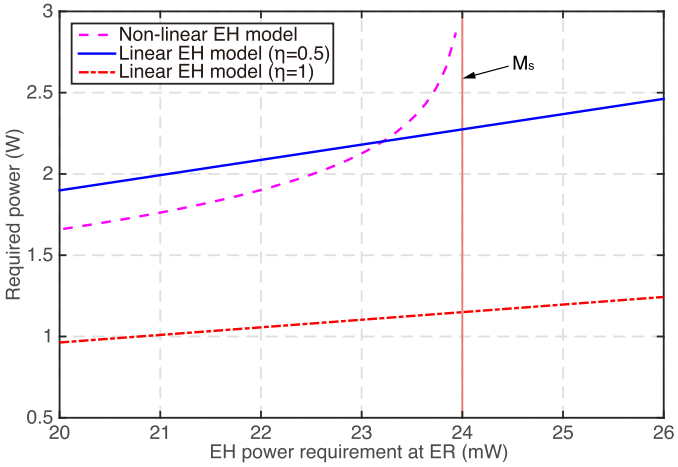

Fig. 9. Required power versus the EH power requirement at ERs under the imperfect CSI assumption.

In order to clearly explain the system optimized under the two EH models, we use Figure 8 to show the feasible sets and the optimal solution of the optimization problems associated with the two models. As is shown, different models construct different feasible sets of the considered problem (12). For the linear EH model, the feasible set mainly depends on the conversion efficiency η. That is, the larger η, the larger feasible set. As for the non-linear EH model, the feasible set mainly depends on the input power level, which indicates that the PF-to-DC conversion efficiency is not a constant anymore, since it takes the practical processing capacity of the rectifying circuit into consideration. As a result, the transmit design based on EH model with large η, e.g., $\eta = 1$, results in a false optimal value, which shall not meet the practical EH requirement and that with small η, e.g., $\eta = 0.5$, results in a non-optimal value which shall consume more power.[7]

With the same parameter setting, the result of the robust design is presented in Figure 9. It can be observed that Figure 9 has the similar shape of Figure 7. The main difference is that in the robust design, more transmit power is consumed compared with the non-robust design.

[7]Note that, Figure 8 just give one example, sometimes the non-linear EH model may consume more power than the linear EH model when $\eta = 0.5$.

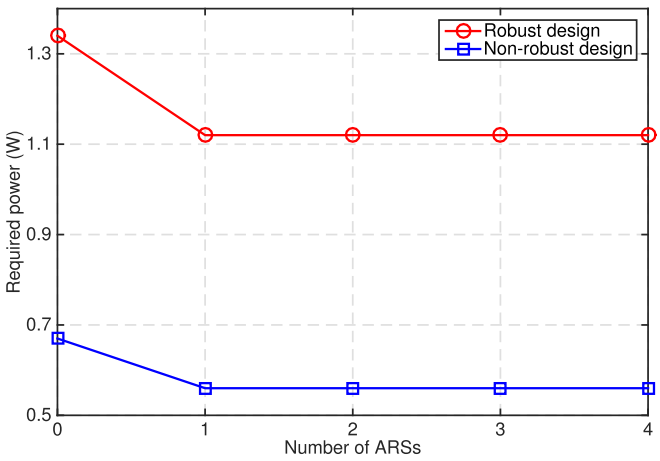

Fig. 10. Required power versus the number of MARSs.

D. AN-Aided vs. MARS-Aided Beamforming Designs

Figure 10 simulates the effect of the numbers of MARSs on the system power requirement. It is observed the power requirement of the non-MARS aided beamforming design (i.e., $L = 0$) is larger than that of the AN-aided beamforming design (i.e., $L = 1$) and the MARS-aided beamforming design (i.e., $L > 1$). Besides, the power requirement of the AN-aided beamforming design is the same with that of the MARS-aided beamforming design, which is consistent with Theorem 1. Moreover, the robust design requires more power than the non-robust one under the same system requirements, which is consistent with the results presented by Figure 5. Although when $L \geq 1$, the number of MARSs has no effect on the system performance, it still makes sense to develop MARS-aided beamforming design. For instance, let us consider a scenario where each signal power is limited [37]. If we cannot generate single optimal ARS with the limited signal power, we can use two or more than two ARSs to replace single ARS so that each signal does not exceed the limited signal power.

VI. Conclusion

This paper studied the transmit beamforming with MARSs for secure SWIPT system under the non-linear EH model. For the considered SWIPT system, in order to achieve the green networks design, the proposed MARS-aided beamforming design was formulated into a power minimization problem, while satisfying the information rate requirement of each IR and the EH requirement of each ER and also making the received SINR at each ER and Eve below a predefined threshold. Both the non-robust and the robust designs were solved by proposed SDR-based solving approaches. Numerous simulation results were presented and demonstrated that the proposed designs are able to achieve better system performance compared with non-MARS aided beamforming designs and transmit designs based on traditional linear EH model. Compared with the non-MARS aided beamforming design, the proposed design consumes less transmit power to achieve the same system performance, especially when there is limited DoF in the system. Compared with traditional linear EH

model, employing the non-linear EH model can avoid false output power at ERs and/or save power consumption at the transmitter, as the real RF-EH circuits are working in the non-linear output field rather than the linear one. These results may be helpful for better understanding the multi-user multi-antenna secure SWIPT system and may also provide some useful insights for future practical secure SWIPT system design.

APPENDIX A
PROOF OF LEMMA 1

Proof: Lemma 1 is proved in the following three cases.

Case 1: Rank $(\mathbf{A}) = 0$ with $\mathbf{A} = \mathbf{0}$. In this case,

$$\det(\mathbf{I} + \mathbf{A}) = \det(\mathbf{I}) = 1 = 1 + \mathrm{Tr}(\mathbf{A}).$$

Case 2: Rank $(\mathbf{A}) = 1$ with $\mathbf{A} \succeq \mathbf{0}$. Let λ be the nonzero eigenvalue of $\mathbf{A}$ (since Rank $(\mathbf{A}) = 1$, $\mathbf{A}$ only have one nonzero eigenvalue). In this case,

$$\det(\mathbf{I} + \mathbf{A}) = 1 + \lambda = 1 + \mathrm{Tr}(\mathbf{A}).$$

Case 3: Rank $(\mathbf{A}) = r > 1$ with $\mathbf{A} \succeq \mathbf{0}$. Let $\lambda_1, \ldots, \lambda_r$ be the nonzero eigenvalue of $\mathbf{A}$. Then

$$\begin{aligned}\det(\mathbf{I} + \mathbf{A}) &= 1 + \prod_{i=1}^{r} \lambda_i \\ &= 1 + \sum_{i=1}^{r} \lambda_i + \sum_{i \neq k}^{r} \lambda_i \lambda_k + \ldots \\ &> 1 + \mathrm{Tr}(\mathbf{A}).\end{aligned}$$

Combining Case 1 and Case 2, we have $\det(\mathbf{I} + \mathbf{A}) = 1 + \mathrm{Tr}(\mathbf{A})$, when Rank $(\mathbf{A}) \leq 1$. From Case 3, we have $\det(\mathbf{I} + \mathbf{A}) > 1 + \mathrm{Tr}(\mathbf{A})$, when Rank $(\mathbf{A}) > 1$. Therefore, Lemma 1 is proved. ∎

APPENDIX B
PROOF OF PROPOSITION 2

Proof: Denote $\mathbf{W}_n^\star$ to be the optimal solution to Problem (24). ${\mathbf{Y}_n}^\star$, $\lambda_n^\star$, $\varphi_k^\star$, $\theta_k^\star$ and $\mu_s^\star$ are the corresponding optimal solution to the dual problem of (24). Then, the KKT equations corresponding to $\mathbf{W}_n^\star$ in (24) are given by

$$\mathbf{I}_{N_\mathrm{T}} - {\mathbf{Y}_n}^\star - \frac{\lambda_n^\star}{\gamma_n}\left(\mathbf{h}_n {\mathbf{h}_n}^H\right) + \mathbf{D} = \mathbf{0} \tag{33a}$$

$$\mathbf{Y}_n^\star \mathbf{W}_n^\star = \mathbf{0} \tag{33b}$$

$$\mathbf{Y}_n^\star \succeq \mathbf{0}, \quad \lambda_n^\star,\ \varphi_s^\star,\ \theta_s^\star,\ \mu_k^\star > 0, \tag{33c}$$

$$\forall n \in \mathcal{N}, \quad \forall k \in \mathcal{K}, \quad \forall s \in \mathcal{S}, \tag{33d}$$

where $\mathbf{D} = \sum_{s=1}^{S}\left(\frac{\theta_s^\star}{\omega_s} - \varphi_s^\star\right)\left(\mathbf{G}_s \mathbf{G}_s^H\right) + \sum_{k=1}^{K} \frac{\mu_k^\star}{\phi_k}\left(\mathbf{g}_k \mathbf{g}_k^H\right)$, which is a PSD matrix.

It is known that

$$\mathrm{Rank}\left({\mathbf{Y}_n}^\star \mathbf{W}_n^\star\right) \geq \mathrm{Rank}\left(\mathbf{Y}_n^\star\right) + \mathrm{Rank}\left(\mathbf{W}_n^\star\right) - N_\mathrm{T} = 0,$$

we have

$$N_\mathrm{T} - \mathrm{Rank}\left(\mathbf{Y}_n^\star\right) \geq \mathrm{Rank}\left(\mathbf{W}_n^\star\right). \tag{34}$$

Based on (34), if Rank $\left(\mathbf{W}_n^\star\right) \neq 0$ and Rank $\left(\mathbf{Y}_n^\star\right) = N_\mathrm{T} - 1$, then Rank $\left(\mathbf{W}_n^\star\right) = 1$ can be proved. In the following parts, we shall prove that Rank $\left(\mathbf{W}_n^\star\right) \neq 0$ and Rank $\left(\mathbf{Y}_n^\star\right) = N_\mathrm{T} - 1$.

According to (14), if Rank $\left(\mathbf{W}_n^\star\right) = 0$, we have

$$0 \geq \mathrm{Tr}\left(\sum\nolimits_{l=1}^{L} \mathbf{h}_n \mathbf{h}_n^H \Sigma_l\right) + \sigma^2.$$

That is, $\Sigma_l \prec \mathbf{0}$ or $\sigma^2 < 0$, which contradicts $\Sigma_l \succeq \mathbf{0}$ and $\sigma^2 > 0$.

Moreover, since $\mathbf{I}_{N_\mathrm{T}} + \mathbf{D}$ is positive definite, we have

$$\mathbf{I}_{N_\mathrm{T}} + \mathbf{D} = \mathbf{B}\mathbf{B}^H, \tag{35}$$

where $\mathbf{B}$ is invertible, i.e., Rank $(\mathbf{B}) = N_\mathrm{T}$.

With (33a) and (35), we can express $\mathbf{Y}_n^\star$ as

$$\begin{aligned}\mathbf{Y}_n^\star &= \mathbf{B}\mathbf{B}^H - \frac{\lambda_n^\star}{\gamma_n}\left(\mathbf{h}_n \mathbf{h}_n^H\right) \\ &= \mathbf{B}\left(\mathbf{I}_{N_\mathrm{T}} - \frac{\lambda_n^\star}{\gamma_n}\mathbf{B}^{-1}\left(\mathbf{h}_n \mathbf{h}_n^H\right)\mathbf{B}^{-H}\right)\mathbf{B}^H.\end{aligned}$$

As a result,

$$\mathrm{Rank}\left(\mathbf{Y}_n^\star\right) = \mathrm{Rank}\left(\mathbf{B}\left(\mathbf{I}_{N_\mathrm{T}} - \frac{\lambda_n^\star}{\gamma}\mathbf{B}^{-1}\left(\mathbf{h}_n \mathbf{h}_n^H\right)\mathbf{B}^{-H}\right)\mathbf{B}^H\right).$$

Since $\mathbf{B}$ is full rank and

$$\mathrm{Rank}\left(\mathbf{Y}_n^\star\right) \leq \min\left\{\mathrm{Rank}(\mathbf{B}), \mathrm{Rank}\left(\mathbf{I}_{N_\mathrm{T}} - \frac{\lambda_n^\star}{\gamma}\mathbf{B}^{-1}\left(\mathbf{h}_n \mathbf{h}_n^H\right)\mathbf{B}^{-H}\right)\right\},$$

we therefore have

$$\mathrm{Rank}\left(\mathbf{Y}_n^\star\right) = \mathrm{Rank}\left(\mathbf{I}_{N_\mathrm{T}} - \frac{\lambda_n^\star}{\gamma_n}\mathbf{B}^{-1}\left(\mathbf{h}_n \mathbf{h}_n^H\right)\mathbf{B}^{-H}\right).$$

Considering that $\mathbf{h}_n$ is not a zero vector (i.e., $\mathbf{h}_n \neq \mathbf{0}$),

$$\mathrm{Rank}\left(\mathbf{I}_{N_\mathrm{T}} - \frac{\lambda_n^\star}{\gamma_n}\mathbf{B}^{-1}\left(\mathbf{h}_n \mathbf{h}_n^H\right)\mathbf{B}^{-H}\right) = N_\mathrm{T} - 1.$$

Thus, Rank $\left(\mathbf{Y}_n^\star\right) = N_\mathrm{T} - 1$. Combining Rank $\left(\mathbf{W}_n^\star\right) \neq 0$ and Rank $\left(\mathbf{Y}_n^\star\right) = N_\mathrm{T} - 1$ with (34), one can infer that Rank $\left(\mathbf{W}_n^\star\right) = 1$. Therefore, Proposition 2 is proved. ∎

REFERENCES

[1] Z. Ding *et al.*, "Application of smart antenna technologies in simultaneous wireless information and power transfer," *IEEE Commun. Mag.*, vol. 53, no. 4, pp. 86–93, Apr. 2015.

[2] D. W. K. Ng and R. Schober, "Secure and green SWIPT in distributed antenna networks with limited backhaul capacity," *IEEE Trans. Wireless Commun.*, vol. 14, no. 9, pp. 5082–5097, Sep. 2015.

[3] K. Xiong, P. Fan, C. Zhang, and K. B. Letaief, "Wireless information and energy transfer for two-hop non-regenerative MIMO-OFDM relay networks," *IEEE J. Sel. Areas Commun.*, vol. 33, no. 8, pp. 1595–1611, Aug. 2015.

[4] X. Lu, P. Wang, D. Niyato, D. I. Kim, and Z. Han, "Wireless network with RF energy harvesting: A contemporary survey," *IEEE Commun. Surveys Tuts.*, vol. 17, no. 2, pp. 757–789, 2nd Quart., 2015.

[5] K. Xiong, C. Chen, G. Qu, P. Y. Fan, and K. B. Letaief, "Group cooperation with optimal resource allocation in wireless powered communication networks," *IEEE Trans. Wireless Commun.*, vol. 16, no. 6, pp. 3840–3853, Jun. 2017.

[6] G. F. Pan, H. J. Lei, Y. Yuan, and Z. G. Ding, "Performance analysis and optimization for SWIPT wireless sensor networks," *IEEE Trans. Commun.*, vol. 65, no. 5, pp. 2291–2302, May 2017.

[7] R. Zhang and C. K. Ho, "MIMO broadcasting for simultaneous wireless information and power transfer," *IEEE Trans. Wireless Commun.*, vol. 12, no. 5, pp. 1989–2001, May 2013.
[8] E. Boshkovska, D. W. K. Ng, N. Zlatanov, and R. Schober, "Practical non-linear energy harvesting model and resource allocation for SWIPT systems," *IEEE Commun. Lett.*, vol. 19, pp. 2082–2085, Dec. 2015.
[9] E. Boshkovska, R. Morsi, D. W. K. Ng, and R. Schober, "Power allocation and scheduling for SWIPT systems with non-linear energy harvesting model," in *Proc. IEEE ICC*, May 2016, pp. 1–6.
[10] Y. J. Dong, Md. J. Hossain, and J. L. Cheng, "Performance of wireless powered amplify and forward relaying over Nakagami-*m* fading channels with non-linear energy harvester," *IEEE Commun. Lett.*, vol. 20, no. 4, pp. 672–675, Apr. 2016.
[11] J. L. Zhang and G. F. Pan, "Outage analysis of wireless-powered relaying MIMO systems with non-linear energy harvesters and imperfect CSI," *IEEE Access*, vol. 4, pp. 7046–7053, Oct. 2016.
[12] E. Boshkovska, D. W. K. Ng, N. Zlatanov, A. Koelpin, and R. Schober, "Robust resource allocation for MIMO wireless powered communication networks based on a non-linear EH model," *IEEE Trans. Wireless Commun.*, vol. 65, no. 5, pp. 1984–1999, Feb. 2017.
[13] K. Xiong, B. Wang, and K. J. R. Liu, "Rate-energy region of SWIPT for MIMO broadcasting under nonlinear energy harvesting," *IEEE Trans. Wireless Commun.*, vol. 16, no. 8, pp. 5147–5161, Aug. 2017.
[14] R. H. Jiang, K. Xiong, P. Y. Fan, Y. Zhang, and Z. D. Zhong, "Optimal design of SWIPT systems with multiple heterogeneous users under non-linear energy harvesting," *IEEE Access*, vol. 5, pp. 11479–11489, Jun. 2017.
[15] H. Liang, C. Zhong, X. Chen, H. Suraweera, and Z. Zhang, "Wireless powered dual-hop multi-antenna relaying systems: Impact of CSI and antenna correlation," *IEEE Trans. Wireless Commun.*, vol. 16, no. 4, pp. 2505–2519, Apr. 2017.
[16] H. Dahrouj and W. Yu, "Coordinated beamforming for the multicell multi-antenna wireless system," *IEEE Trans. Wireless Commun.*, vol. 9, no. 5, pp. 1748–1759, May 2010.
[17] X. Chen, D. W. K. Ng, W. H. Gerstacker, and H. H. Chen, "A survey on multiple-antenna techniques for physical layer security," *IEEE Commun. Surveys Tuts.*, vol. 19, no. 2, pp. 1027–1053, 2nd Quart., 2017.
[18] R. Feng, Q. Li, Q. Zhang, and J. Qin, "Robust secure transmission in MISO simultaneous wireless information and power transfer system," *IEEE Trans. Veh. Technol.*, vol. 64, no. 1, pp. 400–405, Jan. 2015.
[19] W.-C. Liao, T.-H. Chang, W.-K. Ma, and C.-Y. Chi, "QoS-based transmit beamforming in the presence of eavesdroppers: An optimized artificial-noise-aided approach," *IEEE Trans. Signal Process.*, vol. 59, no. 3, pp. 1202–1216, Mar. 2011.
[20] Q. Li and W.-K. Ma, "Spatially selective artificial-noise aided transmit optimization for MISO multi-eves secrecy rate maximization," *IEEE Trans. Signal Process.*, vol. 61, no. 10, pp. 2704–2717, May 2013.
[21] W. Mei, Z. Chen, and C. Huang, "Robust artificial-noise aided transmit design for multi-user MISO systems with integrated services," in *Proc. IEEE ICASSP*, May 2016, pp. 3856–3860.
[22] F. Wang, C. Xu, Y. Huang, X. Wang, and X. Gao, "REEL-BF design: Achieving the SDP sbound for downlink beamforming with arbitrary shaping constraints," *IEEE Trans. Signal Process.*, vol. 65, no. 10, pp. 2672–2685, May 2017.
[23] B. Li, Z. Fei, and H. Chen, "Robust artificial noise-aided secure beamforming in wireless-powered non-regenerative relay networks," *IEEE Access*, vol. 4, pp. 7921–7929, Nov. 2016.
[24] L. Liu, R. Zhang, and K.-C. Chua, "Secrecy wireless information and power transfer with MISO beamforming," *IEEE Trans. Signal Process.*, vol. 62, no. 7, pp. 1850–1863, Apr. 2014.
[25] D. W. K. Ng, E. S. Lo, and R. Schober, "Robust beamforming for secure communication in systems with wireless information and power transfer," *IEEE Trans. Wireless Commun.*, vol. 13, no. 8, pp. 4599–4615, Aug. 2014.
[26] H. Y. Zhang, C. G. Li, Y. M. Huang, and L. X. Yang, "Secure beamforming design for SWIPT in MISO broadcast channel with confidential messages and external eavesdroppers," *IEEE Trans. Wireless Commun.*, vol. 15, no. 11, pp. 7807–7819, Sep. 2016.
[27] F. H. Zhou, Z. Li, J. L. Cheng, Q. W. Li, and J. B. Si, "Robust AN-aided beamforming and power splitting design for secure MISO cognitive radio with SWIPT," *IEEE Trans. Wireless Commun.*, vol. 16, no. 4, pp. 2450–2464, Mar. 2017.
[28] Z. Y. Zhu, Z. Chu, N. Wang, S. Huang, Z. Y. Wang, and I. Lee, "Beamforming and power splitting designs for AN-aided secure multi-user MIMO SWIPT systems," *IEEE Trans. Inf. Forensics Security*, vol. 12, no. 12, pp. 2861–2874, Dec. 2017.
[29] A. Salem, K. A. Hamdi, and K. M. Rabie, "Physical layer security with RF energy harvesting in AF multi-antenna relaying networks," *IEEE Trans. Commun.*, vol. 64, no. 7, pp. 3025–3038, Jul. 2016.
[30] M. Tian, X. Huang, Q. Zhang, and J. Qin, "Robust AN-aided secure transmission scheme in MISO channels with simultaneous wireless information and power transfer," *IEEE Signal Process. Lett.*, vol. 22, no. 6, pp. 723–727, Jun. 2015.
[31] W. D. Mei, B. Fu, L. X. Li, Z. Chen, and C. Huang, "Artificial-noise aided transmit design for multi-user MISO systems with service integration and energy harvesting," in *Proc. IEEE ICC*, May 2016, pp. 219–225.
[32] M. Zhang, Y. Liu, and R. Zhang, "Artificial noise aided secrecy information and power transfer in OFDMA systems," *IEEE Trans. Wireless Commun.*, vol. 15, no. 4, pp. 3085–3096, Apr. 2016.
[33] A. Mukherjee and A. L. Swindlehurst, "Detecting passive eavesdroppers in the MIMO wiretap channel," in *Proc. IEEE ICASSP*, Mar. 2012, pp. 2809–2812.
[34] Z.-Q. Luo, J. F. Sturm, and S. Zhang, "Multivariate nonnegative quadratic mappings," *SIAM J. Optim.*, vol. 14, no. 4, pp. 1140–1162, 2004.
[35] S. Boyd and L. Vandenberghe, *Convex Optimization*. Cambridge, U.K.: Cambridge Univ. Press, 2004.
[36] Z.-Q. Luo, W.-K. Ma, A. M.-C. So, Y. Ye, and S. Zhang, "Semidefinite relaxation of quadratic optimization problems," *IEEE Signal Process. Mag.*, vol. 27, no. 3, pp. 20–34, May 2010.
[37] W.-C. Li, T.-H. Chang, C. Lin, and C.-Y. Chi, "Coordinated beamforming for multiuser MISO interference channel under rate outage constraints," *IEEE Trans. Signal Process.*, vol. 61, no. 5, pp. 1087–1103, Mar. 2013.

Yang Lu received the B.E. degrees from the School of Science, Beijing Jiaotong University (BJTU), Beijing, China, in 2014. He is currently pursuing the Ph.D. degree with the School of Computer and Information Technology, BJTU. His current research interests include the energy efficient communication system design, handover in high-speed railway communication systems, and convex optimization in wireless communications.

Ke Xiong (M'14) received the B.S. and Ph.D. degrees from Beijing Jiaotong University (BJTU), Beijing, China, in 2004 and 2010, respectively. From 2010 to 2013, he was a Post-Doctoral Research Fellow with the Department of Electrical Engineering, Tsinghua University, Beijing. Since 2013, he has been a Lecturer and an Associate Professor with BJTU. From 2015 to 2016, he was a Visiting Scholar with the University of Maryland at College Park, College Park, MD, USA. He is currently a Full Professor with the School of Computer and Information Technology, BJTU. He has published over 100 academic papers in referred journals and conferences.

His current research interests include wireless cooperative networks, wireless powered networks, and network information theory. He is a member of the China Computer Federation and also a Senior Member of the Chinese Institute of Electronics. He also served as the Session Chair for the IEEE GLOBECOM 2012, the IET ICWMMN 2013, the IEEE ICC 2013, the ACM MOMM 2014, and the Publicity and Publication Chair for the IEEE HMWC 2014, and also the TPC Co-Chair of the IET ICWMMN 2017. He serves as an Associate Editor-in-Chief of the Chinese journal *New Industrialization Strategy* and an Editor of the *Computer Engineering and Software*. In 2017, he served as a Leading Editor of the Special issue Recent Advances in Wireless Powered Communication Networks for the *EURASIP Journal on Wireless Communications and Networking* and a Guest Editor of the Special issue Recent Advances in Cloud-Aware Mobile Fog Computing for the *Wireless Communiucations and Mobile Computing*. He currently serves as a reviewer of over 15 international journals, including the IEEE TRANSACTIONS ON SIGNAL PROCESSING, the IEEE TRANSACTIONS ON WIRELESS COMMUNICATIONS, the IEEE TRANSACTIONS ON COMMUNICATIONS, the IEEE TRANSACTIONS ON VEHICULAR TECHNOLOGY, the IEEE COMMUNICATION LETTERS, the IEEE SIGNAL PROCESSING LETTERS and the IEEE WIRELESS COMMUNICATION LETTERS.

Pingyi Fan (M'03–SM'09) received the B.S. degree from the Department of Mathematics, Hebei University, in 1985, the M.S. degree from the Department of Mathematics, Nankai University, in 1990, and the Ph.D. degree from the Department of Electronic Engineering, Tsinghua University, Beijing, China, in 1994. He is currently a Professor with the Department of EE, Tsinghua University. From 1997 to 1998, he visited The Hong Kong University of Science and Technology as a Research Associate. From 1998 to 1999, he visited the University of Delaware, Newark, DE, USA, as Research Fellow. In 2005, he visited NICT of Japan as a Visiting Professor. From 2005 to 2014, he visited The Hong Kong University of Science and Technology several times. From July 2011 to September 2011, he was a Visiting Professor with the Institute of Network Coding, The Chinese University of Hong Kong.

His main research interests include B5G technology in wireless communications, such as MIMO and OFDMA, network coding, network information theory, and big data analysis. He is an Overseas Member of the IEICE. He has served many international conferences, including as the General Co-Chair of the IEEE VTS HMWC 2014, the TPC Co-Chair of the IEEE International Conference on Wireless Communications, Networking and Information Security (WCNIS 2010), and as a TPC member of the IEEE ICC, Globecom, WCNC, VTC, and Inforcom. He has received some academic awards, including the IEEE Globecom 2014 Best Paper Award, the IEEE WCNC 2008 Best Paper Award, the ACM IWCMC 2010 Best Paper Award, and the IEEE ComSoc Excellent Editor Award for the IEEE TRANSACTIONS ON WIRELESS COMMUNICATIONS in 2009. He has served as an Editor for the IEEE TRANSACTIONS ON WIRELESS COMMUNICATIONS, the *International Journal of Ad Hoc and Ubiquitous Computing* (Inderscience), and the *Journal of Wireless Communication and Mobile Computing* (Wiley). He is also a reviewer of over 30 international journals, including 20 IEEE journals and eight EURASIP journals.

Zhangdui Zhong (SM'16) received the B.E. and M.S. degrees from Beijing Jiaotong University, Beijing, China, in 1983 and 1988, respectively. He is currently a Professor and an Advisor of Ph.D. candidates with Beijing Jiaotong University, where he is also a Chief Scientist with the State Key Laboratory of Rail Traffic Control and Safety. He is also the Director of the Innovative Research Team, Ministry of Education, Beijing, and a Chief Scientist with the Ministry of Railways, Beijing. He has authored or co-authored seven books, five invention patents, and over 200 scientific research papers in his research area. His interests include wireless communications for railways, control theory and techniques for railways, and GSM-R systems. His research has been widely used in railway engineering, such as at the Qinghai-Xizang Railway, the Datong-Qinhuangdao Heavy Haul Railway, and many high-speed railway lines in China. He is an Executive Council Member of the Radio Association of China, Beijing, and a Deputy Director of the Radio Association, Beijing. He received the MaoYiSheng Scientific Award of China, the ZhanTianYou Railway Honorary Award of China, and the Top 10 Science/Technology Achievements Award of Chinese Universities.

Khaled Ben Letaief (S'85–M'86–SM'97–F'03) received the Ph.D. degree from Purdue University, IN, USA. He is a Chair Professor and a Provost of HBKU, a newly established research-intensive university in Qatar. He has served as the HKUST Dean of Engineering from 2009 to 2015. Under his leadership, the HKUST School of Engineering has not only transformed its education and scope and produced very high caliber scholarship, it has also actively pursued knowledge transfer and societal engagement in broad contexts. It has also dazzled in international rankings.

He is a world-renowned leader in wireless communications and networks. In these areas, he has over 500 journal and conference papers and given invited keynote talks and also courses all over the world. He has made six major contributions to the IEEE Standards along with 13 patents. He is a Founding Editor-in-Chief of the IEEE TRANSACTIONS ON WIRELESS COMMUNICATIONS and was instrumental in organizing many IEEE flagship conferences and serving in many leadership positions, including the IEEE ComSoc Vice-President for Technical Activities and the IEEE ComSoc Vice-President for Conferences.

Dr. Letaief is an ISI Highly Cited Researcher and a HKIE Fellow. He was a recipient of six teaching awards and 12 IEEE best paper awards, including the 2007 IEEE Joseph LoCicero Award, the 2009 IEEE Marconi Prize Award, the 2010 Purdue Outstanding Electrical and Computer Engineer Award, the 2011 IEEE Harold Sobol Award, and the 2011 IEEE Wireless Communications Technical Committee Recognition Award.